CHEMICAL APPLICATIONS OF NUCLEAR MAGNETIC DOUBLE RESONANCE

JOHN D. BALDESCHWIELER AND EDWARD W. RANDALL*

Department of Chemistry, Harvard University, Cambridge 38, Massachusetts

Received January 17, 1962

CONTENTS

I. Introduction 82
A. Scope of the Review 82
B. Development of the Field 82
C. Nomenclature 82
II. Theory of Double Resonance 82
A. Quantum Mechanical Analysis Neglecting Relaxation Effects 82
1. The Hamiltonian in a Rotating Coördinate System 82
2. The AX System 83
3. The A_3X System 85
4. A Single Nucleus of Spin 1/2 86
5. The AB System 87
B. Nuclear Overhauser Effects 87
C. Density Matrix Treatment 88
III. General Applications 89
A. Effects in the Limit of Large Amplitudes of $\mathbf{H}_2$ 89
1. Spin Decoupling 89
2. The Measurement of Chemical Shifts by Double Resonance 90
B. Effects for Intermediate Amplitudes of $\mathbf{H}_2$ 90
1. Determination of the Amplitude of $\mathbf{H}_2$ 90
2. Effects of Sweeping Magnetic Field 90
3. Relative Signs of Coupling Constants 92
4. Measurement of Small Relative Chemical Shifts 93
5. Measurement of Relaxation Times and Exchange Rates 93
IV. Instrumentation 93
A. Nuclei with Very Different Magnetogyric Ratios 93
1. Locked Oscillator System 93
2. Audio-frequency Modulated Crystal Oscillator 94
3. Audio-frequency Modulated Frequency Divider 94
B. Nuclei with Nearly Equal Magnetogyric Ratios 94
1. Locked Oscillator System 94
2. Field and Frequency Modulation 94
V. Specific Applications 95
A. H^1–$\{H^1\}$ 95
B. H^1-$\{D^2\}$ 100
C. H^1–$\{B^{11}\}$ 101
D. H^1–$\{C^{13}\}$ 102
E. H^1–$\{N^{14}\}$ 102
1. Amides 102
a. Formamide 102
b. N-Methylformamide 103
c. N,N-Dimethylformamide 104
d. Acetamides 104
e. N^{14} Chemical Shifts 104
2. Pyridine and Pyridinium Ion 105
3. Pyrrole 105
4. Ammonia and the Ammonium Ion 106
F. H^1–$\{N^{15}\}$ 106
G. H^1–$\{F^{19}\}$ 106
H. H^1–$\{Al^{27}\}$ 106
I. H^1–$\{P^{31}\}$ 106
J. H^1–$\{Pb^{207}\}$ 106
K. B^{11}–$\{B^{10}\}$ 107
L. C^{13}–$\{H^1\}$ 107

* Chemistry Department, Queen Mary College, University of London, London, E 1, England.

M. C^{13}–{F^{19}} 107
N. F^{19}–{N^{14}} 107
O. F^{19}–{P^{31}} 108
P. Sn^{119}–{H^1} 108
VI. References 108

I. INTRODUCTION

A. SCOPE OF THE REVIEW

Double resonance refers to the general type of spectroscopic experiment in which a system is simultaneously irradiated at two different frequencies. Only nuclear magnetic double resonance is considered in this review. In a nuclear magnetic double resonance experiment, transitions between the energy levels of a nuclear spin system in a magnetic field are studied in the presence of two oscillatory radio-frequency fields. Other types of double resonance experiments, such as simultaneous nuclear and electron spin resonance, are outside the scope of the review. The discussion is further limited to high-resolution studies with liquids. Studies on gases and solids, and the use of pulse and transient techniques are not considered in the review.

B. DEVELOPMENT OF THE FIELD

The double resonance technique was first suggested by Bloch (19). Bloom and Shoolery (22) gave an approximate theoretical treatment for the case of two nuclei of spin 1/2 each, and showed that the theory described the main features of the double resonance spectrum of F^{19} and P^{31} in Na_2PO_3F. A full description of the effect of double resonance on a general spin system was given by Bloch (20). Anderson (8) then applied double resonance techniques to determine the strength of an oscillatory field as suggested by Bloch (20). He further verified that the technique could be used to collapse the multiplet structure arising from the coupling of the spins of protons which differ in chemical shift.

Nuclear magnetic double resonance has had widest application as an aid in the analysis of n.m.r. spectra. In the limit of a large amplitude for one of the oscillatory fields, the multiplet structure arising from the coupling of certain nuclei can be made to disappear (20), and the spins of these nuclei are decoupled from the remainder of the spin system. The complicating effects in n.m.r. spectra arising from the interactions of nuclei with large spin quantum numbers and short relaxation times can thus often be removed by double resonance. Double resonance methods have also been applied to the measurement of chemical shifts (84, 14, 102), and to the determination of the relative signs of coupling constants (32, 56). The theory of double resonance given in Section II of this review shows that in addition to the above uses, there is a variety of other applications of chemical interest for intermediate amplitudes of the oscillatory fields. Some of these applications are reviewed in Sections III and V.

C. NOMENCLATURE

The nuclear magnetic double resonance experiment is performed by applying a strong oscillatory field $\mathbf{H}_2$, of frequency ω_2 near the resonance frequency of one type of nucleus. Transitions of other nuclei in the spin system then are studied with a weak oscillatory field, $\mathbf{H}_1$, of frequency ω_1. The field $\mathbf{H}_2$ is assumed to be strong in the sense that $\gamma_i^2 H_2^2 T_1 T_2 \gg 1$, and $\mathbf{H}_1$ is weak in the sense that $\gamma_i^2 H_1^2 T_1 T_2 \ll 1$ (67). In the following theoretical development, nuclear spin systems will be considered as AX, A_3X, AB and so forth following the usual convention (70). Where possible, the frequency of the strong oscillatory field, ω_2 is considered to be close to the resonance frequency of nucleus X or B, while the transitions of the A nucleus are studied with $\mathbf{H}_1$. A convenient notation used in this review for describing a double resonance experiment is: A–{X}, where the frequency of the strong oscillatory field is close to the resonance frequency of the nucleus in braces, while the other nucleus is studied with the weak field, $\mathbf{H}_1$.

The term "decoupling" is used in this review to refer only to the collapse of spin multiplets by nuclear magnetic double resonance. Other effects such as short relaxation times or chemical exchange also cause the collapse of spin multiplets when the rate of reorientation of the nuclear spin is appreciably greater than the coupling constants between nuclei. These various processes might be expected to be similar; the effect of a double resonance experiment has been described as "nuclear stirring" for example. However, the collapse of multiplet structure in a double resonance experiment has a different origin and terms such as "nuclear stirring" will not be used (2).

II. THEORY OF DOUBLE RESONANCE

A. QUANTUM MECHANICAL ANALYSIS NEGLECTING RELAXATION EFFECTS

1. *The Hamiltonian in a Rotating Coördinate System (2, 12)*

The nuclear spin system is assumed to be in a static magnetic field, $\mathbf{H}_0 = H_0\mathbf{k}$, which lies in the positive z direction. In addition, the spin system interacts with the two fields $\mathbf{H}_1$ and $\mathbf{H}_2$, which oscillate along the x axis, where $\mathbf{H}_1 = 2H_1 \cos \omega_1 t\mathbf{i}$ and $\mathbf{H}_2 = 2H_2 \cos \omega_2 t\mathbf{i}$. It is assumed that each oscillating field can be described

as a pair of counter-rotating fields, and that only the component rotating either with the frequency $-\omega_1$, or $-\omega_2$, is effective in inducing transitions. The error involved in this procedure is negligible when the oscillatory fields are small in comparison with the static field (21, 79). In the nuclear magnetic double resonance experiment, as in the usual high-resolution n.m.r. experiment, the amplitudes of both the weak and strong oscillatory fields are small in comparison with H_0. The nuclear spin system is thus assumed to lie in a total magnetic field given by

$$\mathbf{H} = H_0\mathbf{k} + (H_1 \cos \omega_1 t + H_2 \cos \omega_2 t)\mathbf{i} - (H_1 \sin \omega_1 t + H_2 \sin \omega_2 t)\mathbf{j} \quad (1)$$

The Hamiltonian for a molecule in the liquid state in the field $\mathbf{H}$ in the laboratory coördinate system is

$$\mathcal{H} = \mathcal{H}^0 + \mathcal{H}'(t) \quad (2)$$

where

$$\mathcal{H}^0 = \sum_i \nu_{0i} I_z(i) + \sum_{i<j} J_{ij}\mathbf{I}(i)\cdot\mathbf{I}(j) \quad (3)$$

$$\mathcal{H}'(t) = \sum_i \nu_{2i}[I_x(i) \cos \omega_2 t - I_y(i) \sin \omega_2 t] + \sum_i \nu_{1i}[I_x(i) \cos \omega_1 t - I_y(i) \sin \omega_1 t] \quad (4)$$

$\nu_{0i} = -\gamma_i H_0/2\pi$
$\nu_{1i} = -\gamma_i H_1/2\pi$
$\nu_{2i} = -\gamma_i H_2/2\pi$
γ_i = magnetogyric ratio of nucleus i including the chemical shift
J_{ij} = spin–spin coupling constant between nuclei i and j in c./s.

The Hamiltonian is given in units of cycles per second (c./s.), and the summations are carried out over all the spins i and j in the molecule. In the laboratory system, the Schrödinger equation is

$$i\dot{\Psi} = 2\pi\mathcal{H}\Psi \quad (5)$$

Since the Hamiltonian is time dependent, it is not possible to obtain time-independent solutions to equation (5). However, the time-dependent terms in H_2 can be removed if the Schrödinger equation is written in a coördinate system that rotates with angular velocity $-\omega_2\mathbf{k}$ (22, 7). The operator for a finite rotation $-\omega_2\mathbf{k}t$ can be written:

$$u = \exp(i\omega_2 I_z t) \quad (6)$$

If the wave function in the rotating coördinate system is defined as $\Psi_R = u\Psi$, the Schrödinger equation can be written in the rotating coördinate system as (78)

$$i\dot{\Psi}_R = 2\pi\mathcal{H}_R\Psi_R \quad (7)$$

where

$$\mathcal{H}_R = \mathcal{H}_R^0 + \mathcal{H}_R'(t) \quad (8)$$

$$\mathcal{H}_R^0 = \sum_i A_i I_z(i) + \sum_{i<j} J_{ij}\mathbf{I}(i)\cdot\mathbf{I}(j) + \sum_i \nu_{2i} I_x(i) \quad (9)$$

$$\mathcal{H}_R'(t) = \sum_i \nu_{1i}[I_x(i) \cos(\omega_1 - \omega_2)t - I_y(i) \sin(\omega_1 - \omega_2)t] \quad (10)$$

$$A_i = (\nu_{0i} + \omega_2/2\pi)$$

In the rotating coördinate system, the time dependence of the Hamiltonian remains only in $\mathcal{H}_R'(t)$. If it is assumed that $\mathcal{H}_R'(t)$ is small with respect to $\mathcal{H}_R^0$, then the solution to equation (7) can be obtained using first-order perturbation theory. The unperturbed Hamiltonian $\mathcal{H}_R^0$ can be solved for its stationary eigenvalues, E_R, and its normalized eigenfunctions, ψ_R.

$$\mathcal{H}_R^0\psi_R = E_R\psi_R \quad (11)$$

The time-dependent perturbation, to first order, then gives the transition probability per unit time, P_{ij}, between states ψ_{Ri} and ψ_{Rj}. The transition probability per unit time is proportional to $|\langle i|\mathcal{H}_R'|j\rangle|^2 g[(\omega_1 - \omega_2) - \omega]$ where $\omega = 2\pi(E_{Ri} - E_{Rj})$, and the function g indicates that the transition probability is large when $\omega_1 - \omega_2$ is close to ω. The relative intensities of the resonances observed in the laboratory system are then assumed (without theoretical justification) to be proportional to these relative transition probabilities in the rotating system (3). The frequency, $\omega_1/2\pi$, at which a transition is observed in the laboratory system is given by

$$\omega_1/2\pi = E_{Ri} - E_{Rj} + \omega_2/2\pi \quad (12)$$

The calculation of the frequencies and relative intensities of absorption for double resonance requires diagonalization of the Hamiltonian $\mathcal{H}_R^0$ in the space of an appropriate complete set of basis functions for the spin system.

2. *The AX System*

The Hamiltonian in the rotating coördinate system for an AX molecule where the nuclei A and X both have spin 1/2 is given by

$$\mathcal{H}_R^0 = A_a I(a) + A_x I_z(x) + J_{ax} I(a)\cdot\mathbf{I}(x) + \nu_{2a} I_x(a) + \nu_{2x} I_x(x) \quad (13)$$

where the subscripts a and x on the terms A, J, and ν refer to nuclei A and X, respectively. The spin-product basis functions, and the diagonal matrix elements of $\mathcal{H}_R^0$ are given in Table I. The terms $\nu_{2a} I_x(a)$, $\nu_{2x} I_x(x)$, and the x and y parts of $J_{ax} I(a)\cdot I(x)$ give rise to off-diagonal matrix elements of $\mathcal{H}_R^0$. The complete matrix, $\mathcal{H}_R^0$, for the AX system is

$$\begin{pmatrix} \mathcal{H}_{R11}^0 & \frac{1}{2}\nu_{2x} & \frac{1}{2}\nu_{2a} & 0 \\ \frac{1}{2}\nu_{2x} & \mathcal{H}_{R22}^0 & \frac{1}{2}J_{ax} & \frac{1}{2}\nu_{2a} \\ \frac{1}{2}\nu_{2a} & \frac{1}{2}J_{ax} & \mathcal{H}_{R33}^0 & \frac{1}{2}\nu_{2x} \\ 0 & \frac{1}{2}\nu_{2a} & \frac{1}{2}\nu_{2x} & \mathcal{H}_{R44}^0 \end{pmatrix}.$$

It is now assumed that $\omega_2/2\pi$ is close to ν_{ox}, the resonance frequency of nucleus X, and $\omega_1/2\pi$ is close to ν_{oa}, the resonance frequency of nucleus A. Furthermore, for an AX system, it is assumed that ν_{oa} is very different from ν_{ox}. Thus, the term A_x will be very small, or even zero if $\omega_2/2\pi$ is exactly equal to the resonance frequency of nucleus X. The term A_a, however, is large, since it equals the difference between $\omega_2/2\pi$ and the resonance frequency of nucleus A.

TABLE I

DIAGONAL MATRIX ELEMENTS FOR THE AX SYSTEM

No (i)	ϕ_i	Diagonal matrix elements, $\mathcal{H}_{Rii}^0$
1	$\alpha\alpha$	$^1/_2A_a + {}^1/_2A_x + {}^1/_4J_{ax}$
2	$\alpha\beta$	$^1/_2A_a - {}^1/_2A_x - {}^1/_4J_{ax}$
3	$\beta\alpha$	$-{}^1/_2A_a + {}^1/_2A_x - {}^1/_4J_{ax}$
4	$\beta\beta$	$-{}^1/_2A_a - {}^1/_2A_x + {}^1/_4J_{ax}$

Off-diagonal elements of $\mathcal{H}_R^0$ in v_{2a} and J_{ax} connect diagonal elements that differ in energy by about A_a. Since A_a is large, these off-diagonal elements can be neglected. The off-diagonal elements in v_{2x}, however, connect diagonal elements differing in energy by only A_x, so that these off-diagonal elements must be considered. With these approximations, the secular determinant becomes

$$\begin{vmatrix} \mathcal{H}_{R11}^0 - E_R & {}^1/_2\, v_{2x} & 0 & 0 \\ {}^1/_2\, v_{2x} & \mathcal{H}_{R22}^0 - E_R & 0 & 0 \\ 0 & 0 & \mathcal{H}_{R33}^0 - E_R & {}^1/_2\, v_{2x} \\ 0 & 0 & {}^1/_2\, v_{2x} & \mathcal{H}_{R44}^0 - E_R \end{vmatrix} = 0 \quad (14)$$

The eigenvalues, E_{Ri}, and the eigenvectors, ψ_{Ri}, are given in Table II, where the notation (12, 14) has been introduced

$$l = [(A_x + {}^1/_2\, J_{ax})^2 + v_{2x}^2]^{1/2} \quad (15)$$

$$m = [(A_x - {}^1/_2\, J_{ax})^2 + v_{2x}^2]^{1/2} \quad (16)$$

$$\theta_l = \cos^{-1}(A_x + {}^1/_2\, J_{ax})/l \quad (17)$$

$$\theta_m = \cos^{-1}(A_x - {}^1/_2\, J_{ax})/m \quad (18)$$

Since only resonances close to the resonance frequency of nucleus A are studied with the weak field H_1, the relative intensities of the observed transitions will be proportional to terms of the type $|\langle\psi_{Ri}|I_x(a)|\psi_{Rj}\rangle|^2$. The relative intensities and ΔE_R values for the allowed transitions are given in Table III. The resonance frequencies of the allowed transitions, $\omega_1/2\pi$, are found from the ΔE_R values from equation (12).

TABLE II

EIGENVALUES AND EIGENVECTORS FOR THE AX SYSTEM

No (i)	Eigenvalues E_{Ri}	Eigenvectors, ψ_{Ri}
1	$^1/_2A_a + {}^1/_2l$	$-\cos\frac{\theta_l}{2}\phi_1 + \sin\frac{\theta_l}{2}\phi_2$
2	$^1/_2A_a - {}^1/_2l$	$\sin\frac{\theta_l}{2}\phi_1 + \cos\frac{\theta_l}{2}\phi_2$
3	$-{}^1/_2A_a + {}^1/_2m$	$-\cos\frac{\theta_m}{2}\phi_3 + \sin\frac{\theta_m}{2}\phi_4$
4	$-{}^1/_2A_a - {}^1/_2m$	$\sin\frac{\theta_m}{2}\phi_3 + \cos\frac{\theta_m}{2}\phi_4$

As in the normal high-resolution n.m.r. experiment, double resonance spectra usually are recorded by changing H_0 with a constant value of ω_1. Using the definitions of A_a, A_x, m, and l, and replacing H_0 by $H_0 + \Delta H_0$, equation (12), for transition (1→3), for example, becomes

TABLE III

ALLOWED TRANSITIONS FOR THE AX SYSTEM

Transition	ΔE_R	Relative intensity
1→3	$-A_a + {}^1/_2(m - l)$	$\cos^2\frac{\theta_l - \theta_m}{2}$
1→4	$-A_a + {}^1/_2(-m - l)$	$\sin^2\frac{\theta_l - \theta_m}{2}$
2→3	$-A_a + {}^1/_2(m + l)$	$\sin^2\frac{\theta_l - \theta_m}{2}$
2→4	$-A_a + {}^1/_2(-m + l)$	$\cos^2\frac{\theta_l - \theta_m}{2}$

$$\Delta H_0 = -{}^1/_2\left\{\left[\left(A_x - \frac{\gamma_x}{\gamma_a}\Delta H_0 - {}^1/_2\, J\right)^2 + v_{2x}^2\right]^{1/2} - \left[\left(A_x - \frac{\gamma_x}{\gamma_a}\Delta H_0 + {}^1/_2\, J\right)^2 + v_{2x}^2\right]^{1/2}\right\} \quad (19)$$

where ΔH_0 is given in cycles per second. For the special case when A_x is equal to zero, this equation can be readily solved for ΔH_0

$$\Delta H_0 = \pm\left\{\frac{4\gamma_a^2 v_{2x}^2 + J^2(\gamma_a^2 - \gamma_x^2)}{4(\gamma_a^2 - \gamma_x^2)}\right\}^{1/2} \quad (20)$$

This result is equivalent to that given by Bloom and Shoolery (22) for "case 2" in which $\omega_2 = \gamma_x H_0$, ω_1 is fixed at $\gamma_a H_0$, and the spectrum is recorded by changing the static magnetic field.

Freeman and Whiffen (33) have given a convenient schematic representation of the calculated lines in the A part of an AX spectrum when ω_2 is near the X resonance frequency, and the spectra are obtained by varying either H_0 or ω_1. The spectra calculated for field and frequency sweep conditions with various values of A_x, and with $v_{2x} = {}^1/_2J$ are shown in Figure 1. These calculated spectra are compared with the double resonance spectra of the AX system dichloroacetaldehyde. The excellent agreement of the observed and calculated double resonance spectra indicates that for this system the elementary theory is a good description of the double resonance process.

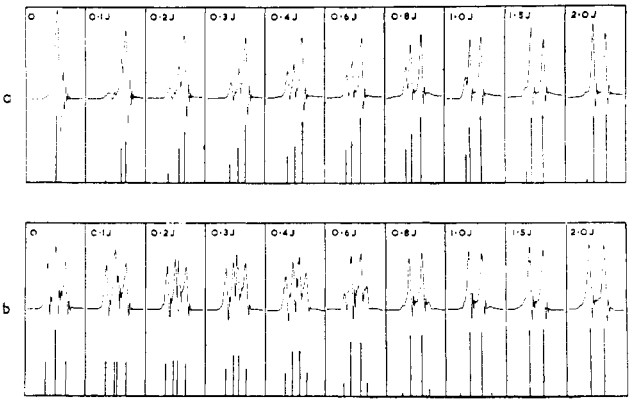

Fig. 1.—The A resonance of the AX system dichloroacetaldehyde for various values of A_x in units of J_{ax}, with $v_{2x} = {}^1/_2J_{ax}$. The calculated and observed spectra are shown for (a) the field-sweep method, and (b) the frequency-sweep method (33).

3. *The A_3X System (12)*

The system A_3X is assumed to include a nucleus X of spin 1, and three equivalent nuclei of spin 1/2, where the resonance frequencies of nuclei A and X are quite different. The Hamiltonian for this molecule in the rotating coördinate system is

$$\mathcal{H}_R^0 = \sum_{i=1}^{3} A_a I_z(i) + A_x I_z(x) + \sum_{i=1}^{3} J_{ax}\mathbf{I}(i)\cdot\mathbf{I}(x) + \sum_{i<j} J_{aa} I(i)\cdot I(j) + \sum_{i=1}^{3} v_{2a} I_x(i) + v_{2x} I_x(x) \quad (21)$$

where the summations are over the three equivalent A nuclei.

It is readily shown that the term $\sum_{i<j} J_{aa} I(i)\cdot I(j)$ commutes with $\mathcal{H}_R^0$, and with the x component of the total nuclear moment. Thus the double resonance spectrum will not depend on terms in the coupling between the equivalent nuclei. These accordingly can be omitted from the total Hamiltonian. If the total angular momentum of the equivalent nuclei is given by

$$\mathbf{K}(a) = \sum_i \mathbf{I}(i) \quad (22)$$

as first suggested by Hahn and Maxwell (37), and Gutowsky, McCall, and Slichter (36), then

$$[\mathcal{H}_R^0, \mathbf{K}^2] = 0 \quad (23)$$

Thus the matrix elements of $\mathcal{H}_R^0$ can be written in a set of basis functions of the type $|K, m_k, m_x\rangle$, following the procedure of Waugh and Dobbs (105). The Hamiltonian then can be written

$$\mathcal{H}_R^0 = A_a K_z(a) + A_x I_z(x) + J_{ax}\mathbf{K}(a)\cdot\mathbf{I}(x) + v_{2a} K_x(a) + v_{2x} I_x(x) \quad (24)$$

Since the z component of the total spin angular momentum F_z does not commute with $\mathcal{H}_R^0$, the secular determinant does not factor in the usual way (68).

It is again assumed that $\omega_2/2\pi$ is close to v_{ox}, and $\omega_1/2\pi$ is close to v_{oa}. Thus as in the AX case, A_x will be zero, or very small, while A_a is large. The terms $v_{2a}K_x(a)$ and $J_{ax}[K_x(a)I_x(a) + K_y(a)I_y(a)]$ connect diagonal elements separated by about A_a, and thus can be neglected. Off-diagonal elements arising from the term $v_{2x}I_x(x)$, however, connect diagonal elements differing by only A_x, and must be considered. With these simplifications the Hamiltonian becomes

$$\mathcal{H}_R^0 = A_a K_z(a) + A_x K_z(x) + J_{ax} K_z(a) I_z(x) + v_{2x} I_x(x) \quad (25)$$

It is also clear that for this Hamiltonian

$$[\mathcal{H}_R^0, K_z] = 0 \quad (26)$$

so that there will be no off-diagonal elements of $\mathcal{H}_R^0$ between basis functions corresponding to different values of K_z. The diagonalization of the Hamiltonian thus requires the solution of three-by-three determinants.

The basis functions of the type $|K, m_k, m_x\rangle$ and the diagonal elements of $\mathcal{H}_R^0$ are given in Table IV. In the approximation that off-diagonal elements in J_{ax} and v_{2a} can be neglected, the only off-diagonal elements of $\mathcal{H}_R^0$ arise from the term $v_{2x}I_x(x)$ in equation (25). The only states connected by $I_x(x)$ are those with m_x equal to (1) and (0); and (0) and (−1), for a given m_k. The magnitude of these elements is $(\sqrt{2}/2)v_{2x}$. A typical three-by-three block of the secular determinant is

$$\begin{vmatrix} \mathcal{H}_{R11}^0 - E_R & (\sqrt{2}/2)v_{2x} & 0 \\ (\sqrt{2}/2)v_{2x} & \mathcal{H}_{R22}^0 - E_R & (\sqrt{2}/2)v_{2x} \\ 0 & (\sqrt{2}/2)v_{2x} & \mathcal{H}_{R33}^0 - E_R \end{vmatrix} = 0 \quad (27)$$

TABLE IV

DIAGONAL MATRIX ELEMENTS FOR A_3X MOLECULE

No.	Basis Function ϕ_i (K, m_k, m_x)			Diagonal elements $\mathcal{H}_{Rii}^0$	E_R
				$K = 3/2$, wt. = 1	
1	3/2	3/2	1	$^3/_2A_a + A_x + {}^3/_2J_{ax}$	$^3/_2A_a + l$
2			0	$^3/_2A_a$	$^3/_2A_a$
3			−1	$^3/_2A_a - A_x - {}^3/_2J_{ax}$	$^3/_2A_a - l$
4		1/2	1	$^1/_2A_a + A_x + {}^1/_2J_{ax}$	$^1/_2A_a + m$
5			0	$^1/_2A_a$	$^1/_2A_a$
6			−1	$^1/_2A_a - A_x - {}^1/_2J_{ax}$	$^1/_2A_a - m$
7		−1/2	1	$-{}^1/_2A_a + A_x - {}^1/_2J_{ax}$	$-{}^1/_2A_a + n$
8			0	$-{}^1/_2A_a$	$-{}^1/_2A_a$
9			−1	$-{}^1/_2A_a - A_x + {}^1/_2J_{ax}$	$-{}^1/_2A_a - n$
10		−3/2	1	$-{}^3/_2A_a + A_x - {}^3/_2J_{ax}$	$-{}^3/_2A_a + o$
11			0	$-{}^3/_2A_a$	$-{}^3/_2A_a$
12			−1	$-{}^3/_2A_a - A_x + {}^3/_2J_{ax}$	$-{}^3/_2A_a - o$
				$K = 1/2$, wt. = 2	
13	1/2	1/2	1	$^1/_2A_a + A_x + {}^1/_2J_{ax}$	$^1/_2A_a + m$
14			0	$^1/_2A_a$	$^1/_2A_a$
15			−1	$^1/_2A_a - A_x - {}^1/_2J_{ax}$	$^1/_2A_a - m$
16		−1/2	1	$-{}^1/_2A_a + A_x - {}^1/_2J_{ax}$	$-{}^1/_2A_a + n$
17			0	$-{}^1/_2A_a$	$-{}^1/_2A_a$
18			−1	$-{}^1/_2A_a - A_x + {}^1/_2J_{ax}$	$-{}^1/_2A_a - n$

The solution of this determinant yields the values of E_R given in Table IV, where

$$l = [(A_x + {}^3/_2\, J_{ax})^2 + v_{2x}^2]^{1/2} \quad (28)$$

$$m = [(A_x + {}^1/_2\, J_{ax})^2 + v_{2x}^2]^{1/2} \quad (29)$$

$$n = [(A_x - {}^1/_2\, J_{ax})^2 + v_{2x}^2]^{1/2} \quad (30)$$

$$o = [(A_x - {}^3/_2\, J_{ax})^2 + v_{2x}^2]^{1/2} \quad (31)$$

The eigenfunctions for the first block in the secular equation can be written

$$\psi_{R1} = {}^1/_2\,(1 + \cos\theta_1)\phi_1 - {}^{\sqrt{2}}/_2 \sin\theta_1\phi_2 + {}^1/_2\,(1 - \cos\theta_1)\phi_3 \quad (32)$$

$$\psi_{R2} = -{}^1/_{\sqrt{2}} \sin\theta_1\phi_1 - \cos\theta_1\phi_2 + {}^1/_{\sqrt{2}} \sin\theta_1\phi_3 \quad (33)$$

$$\psi_{R3} = {}^1/_2\,(1 - \cos\theta_1)\phi_1 + {}^{\sqrt{2}}/_2 \sin\theta_1\phi_2 + {}^1/_2\,(1 + \cos\theta_1)\phi_3 \quad (34)$$

where

$$\theta_1 = \cos^{-1}(A_x + {}^3/_2\, J_{ax})/l \quad (35)$$

$$\theta_m = \cos^{-1}(A_x + {}^1/_2\, J_{ax})/m \quad (36)$$

$$\theta_n = \cos^{-1}(A_x - {}^1/_2\, J_{ax})/n \quad (37)$$

$$\theta_0 = \cos^{-1}(A_x - {}^3/_2\, J_{ax})/o \quad (38)$$

The eigenfunctions for the other blocks in the secular equation will be similar functions in the angles θ_m, θ_n, and θ_0. Since only transitions close to the resonance

frequency of the A nuclei are being studied, only those transitions are allowed for which $\Delta m_k = \pm 1$. The transition probabilities are proportional to terms of the type

$$|\langle\psi_{Ri}(\theta_l)|(K_x(a)|\psi_{Rj}(\theta_m)\rangle|^2$$

There will be in general nine allowed transitions for each pair of m_k values. The relative intensities and the ΔE_R values for the allowed transitions of the type $m_k = 3/2 \rightarrow m_k = 1/2$ are given in Table V. The values of ΔE_R for transitions of the type $m_k = 1/2 \rightarrow m_k = -1/2$ and $m_k = -1/2 \rightarrow m_k = -3/2$ are obtained by replacing m and l in Table V by the other appropriate constants n and o. The relative intensities of transitions of the type $m_k = 1/2 \rightarrow m_k = -1/2$ are obtained by multiplying the relative intensities given in Table V by 2 and replacing θ_m and θ_l by θ_n and θ_m, respectively. The relative intensities for the $m_k = -1/2 \rightarrow m_k = -3/2$ transitions are obtained by replacing θ_m and θ_l in Table V by θ_0 and θ_m, respectively. The frequencies of the allowed transitions in the laboratory coördinate system are found from the ΔE_R values using equation (12).

TABLE V

ALLOWED TRANSITIONS FOR THE A_3X SPECIES

Transition	$R = 3/2$, $m_K = 3/2 \rightarrow m_K = 1/2$ ΔE_R	Relative intensity
1→4	$-A_x + m - l$	$1/4[1 + \cos(\theta_m - \theta_l)^2$
1→5	$-A_x - l$	$1/2 \sin^2(\theta_m - \theta_l)$
1→6	$-A_x - m - l$	$1/4[1 - \cos(\theta_m - \theta_l)]^2$
2→4	$-A_x + m$	$1/2 \sin^2(\theta_m - \theta_l)$
2→5	$-A_x$	$\cos^2(\theta_m - \theta_l)$
2→6	$-A_x - m$	$1/2 \sin^2(\theta_m - \theta_l)$
3→4	$-A_x + m + l$	$1/4[1 - \cos(\theta_m - \theta_l)]^2$
3→5	$-A_x + l$	$1/2 \sin^2(\theta_m - \theta_l)$
3→6	$-A_x - m + l$	$1/4[1 + \cos(\theta_m - \theta_l)]^2$

If the double resonance spectrum is recorded by changing the static magnetic field with a constant value of ω_1, the values of ΔH_0 at which the transitions occur can be calculated from equation (12) by using the definitions of A_x, A_a, l, m, n, o, and replacing H_0 by $H_0 + \Delta H_0$. For transition 1→4 of the type $m_k = 3/2 \rightarrow m_k = 1/2$, equation (12) becomes

$$\Delta H_0 = -\left[(A_x - \frac{\gamma_x}{\gamma_a}\Delta H_0 + 1/2\, J_{ax})^2 + \gamma_{2x}{}^2\right]^{1/2} + \left[(A_x - \frac{\gamma_x}{\gamma_a}\Delta H_0 + 3/2\, J_{ax})^2 + v_{2x}{}^2\right]^{1/2} \quad (39)$$

where ΔH_0 is in cycles per second. The solution of equation (39) for ΔH_0 is similar to the solution of equation (19) if A_x is equal to zero. When A_x is not equal to zero, and γ_x/γ_a is much less than one, the solution of equation (39) can be effected by an iterative procedure.

4. *A Single Nucleus of Spin 1/2*

The effect of irradiating at two different frequencies a molecule containing a single nucleus of spin 1/2 has been described by Bloch (20) and Anderson (8). From equation (9), the Hamiltonian for a single nucleus A of spin 1/2 in the rotating coördinate system is

$$\mathcal{H}_R{}^0 = A_a I_z(a) + v_{2a} I_x(a) \quad (40)$$

where the subscript a refers to nucleus A. The matrix elements of $\mathcal{H}_R{}^0$ are easily given in the set of basis functions α and β for the nuclear spin. The secular determinant for this case is

$$\begin{vmatrix} 1/2\, A_a - E_R & 1/2\, v_{2a} \\ 1/2\, v_{2a} & -1/2\, A_a - E_R \end{vmatrix} = 0 \quad (41)$$

The solution of this determinant gives

$$E_R = \pm 1/2\, [A_a{}^2 + v_{2a}{}^2]^{1/2} \quad (42)$$

$$\Delta E_R = -[A_a{}^2 + v_{2a}{}^2]^{1/2} \quad (43)$$

The probability of transition between two states ψ_{R_i} and ψ_{R_j} induced by the time-dependent perturbation $\mathcal{H}_R'(t)$ is appreciable when (88)

$$\Delta E_{Rij} = \pm \frac{\omega_1 - \omega_2}{2\pi} \quad (44)$$

When ΔE_{Rij} is large, only the positive sign in equation (44) leads to resonances in the region where $\omega_1/2\pi \sim \nu_{0a}$ in the laboratory system. However, when ΔE_{Rij} is very small, both the positive and negative signs in equation (44) lead to resonances in a region of interest. Thus if $\omega_2/2\pi \sim \nu_{0a}$, then ΔE_{Rij} is small, and from equations (43) and (44) for a single spin A

$$\frac{\omega_1}{2\pi} = \frac{\omega_2}{2\pi} \pm \left[\left(\nu_{0a} + \frac{\omega_2}{2\pi}\right)^2 + v_{2a}{}^2\right]^{1/2} \quad (45)$$

If the resonances are observed by changing the magnetic field with fixed values of ω_1 and ω_2 two resonances will be observed when $|(\omega_1 - \omega_2)/2\pi| > |v_{2a}|$.

The relative intensities and line widths of the two resonances have been derived by Anderson (8) from the Bloch phenomenological equations (18), and by Bloch (20) starting with the general density matrix description of the spin system. For a single spin of 1/2 the two methods are equivalent (104).

It is important to note that the resonance obtained at a value of $\omega_1/2\pi$ calculated with the positive sign in equation (45) appears "below the line." The intensity of this resonance is opposite in sign to the intensity of the usual absorption mode signal. Double resonance spectra for the protons in water at various values of $(\omega_1 - \omega_2)/2\pi$ are shown in Figure 2.

If the weak radio frequency field $\mathbf{H}_1$ is obtained by modulation of $\mathbf{H}_0$ at an audio-frequency $\omega' = \omega_1 - \omega_2$, the resonance condition of the sideband is given by (8)

$$\left(\frac{\omega'}{2\pi}\right)^2 = \left(\nu_{0a} + \frac{\omega_2}{2\pi}\right)^2 + v_{2a}{}^2 \quad (46)$$

Equation (46) is satisfied for two values of ν_{0a} providing $|\omega'/2\pi| > |v_{2a}|$

$$\nu_{0a} = \pm\left[\left(\frac{\omega'}{2\pi}\right)^2 - v_{2a}{}^2\right]^{1/2} - \frac{\omega_2}{2\pi} \quad (47)$$

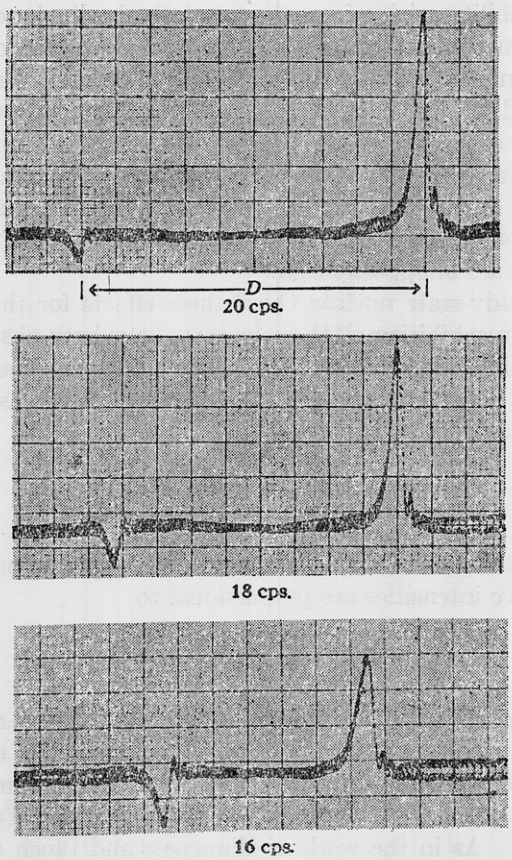

Fig. 2.—Double resonance spectra of protons in water at various values of $(\omega_1 - \omega_2)/2\pi$. The spacing of the two signals is given by $D = \nu^{+}_{oa} - \nu^{-}_{oa}$ (see Section III-B-1) (8).

From these results it is evident that the usual method of calibrating n.m.r. spectra with audio-frequency sidebands will give erroneous results for small values of $\omega'/2\pi$ or large values of ν_{2a} (24, 102, 30, 33). Chemical shifts measured by double resonance methods also must be corrected for this effect (30).

5. *The AB System*

An AB system is defined as a set of nuclear spins for which the difference in the A and B resonance frequencies, $\nu_{oa} - \nu_{ob}$ is comparable to J_{ab}, ν_{2a}, or ν_{2b}. It is important to note that in a double resonance experiment, ν_{2a} and ν_{2b} are often far larger than J_{ab}. Hence, a system that could be treated in the AX approximation for a usual high-resolution n.m.r. experiment might still have $\nu_{oa} - \nu_{ob}$ comparable to ν_{2a} or ν_{2b} in a double resonance experiment. The results for the AX treatment thus can be applied only with considerable caution to double resonance experiments which involve nuclei of the same kind differing only in chemical shift (30, 33, 59).

The Hamiltonian for an AB molecule, where nuclei A and B both have spin 1/2, is similar to that for the AX system given in equation (3), where the subscript x is replaced by b. The complete matrix of the Hamiltonian is

$$\begin{pmatrix} \mathcal{H}_{R11}{}^0 & \frac{1}{2}\nu_{2b} & \frac{1}{2}\nu_{2a} & 0 \\ \frac{1}{2}\nu_{2b} & \mathcal{H}_{R22}{}^0 & \frac{1}{2}J_{ab} & \frac{1}{2}\nu_{2a} \\ \frac{1}{2}\nu_{2a} & \frac{1}{2}J_{ab} & \mathcal{H}_{R33}{}^0 & \frac{1}{2}\nu_{2b} \\ 0 & \frac{1}{2}\nu_{2a} & \frac{1}{2}\nu_{2b} & H_{R44}{}^0 \end{pmatrix}$$

Since ν_{oa} and ν_{ob} are nearly equal for an AB system, both A_a and A_b will be small. Thus, off-diagonal elements in ν_{2a}, ν_{2b}, and J_{ab} must be considered. The secular determinant, then, is not factorable as in the AX case.

For the AB case, all six transitions are allowed between the stationary solutions E_R in the rotating coordinate system. In addition, since ω_1 will be very close to ω_2, all the ΔE_R values will be small, and both signs in equation (44) must be considered in calculating the resonance frequencies in the laboratory system. Six positive and six negative signals are possible in either fixed field or fixed frequency experiments.

B. NUCLEAR OVERHAUSER EFFECTS

The relative intensities of transitions in a double resonance experiment depend not only on the relative transition probabilities between the stationary states of the system, but also on the population distribution among the states. In general, even the populations of states that are not directly affected by the strong field $\mathbf{H}_2$ deviate from the value corresponding to thermal equilibrium in the absence of $\mathbf{H}_2$. This general Overhauser (64) effect depends on the various relaxation processes between the stationary states of the system, and represents the readjustment of all the populations to new stationary values in the presence of $\mathbf{H}_2$.

The effects of various relaxation processes on the population distribution in a system of two spins of 1/2 each have been described by Abragam (1). Solomon (97) and Solomon and Bloembergen (98) have described the nuclear Overhauser effect for an AX system where both nuclei have spin 1/2. The energy level diagram for an AX system where the magnetogyric ratios of both nuclei are positive and spin–spin coupling can be neglected is shown in Figure 3. The four unperturbed states are described as $\alpha\alpha$, $\alpha\beta$, $\beta\alpha$, and $\beta\beta$ in

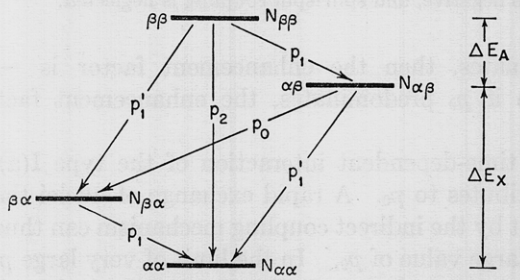

Fig. 3.—Energy level diagram for an AX system where the magnetogyric ratios of both nuclei are positive and spin–spin coupling is neglected.

the nuclear spins, the energy difference between states differing in the spin of nucleus X is ΔE_x, and the energy difference between states differing in the spin of nucleus A is ΔE_A. The constants p_0, p_1, p_1', and p_2 are the transition probabilities between the eigenstates of the AX system. The populations of the various states are given by $N_{\alpha\alpha}$, $N_{\alpha\beta}$, $N_{\beta\alpha}$, and $N_{\beta\beta}$. The rates of change of the populations of the various energy levels in the presence of $\mathbf{H}_2$ can be written in terms of the transition probabilities between the various states and the amplitude of $\mathbf{H}_2$ (1). The steady-state solution of the resulting set of differential equations gives the stationary populations of the states in the presence of $\mathbf{H}_2$.

In the absence of $\mathbf{H}_2$, population differences $N_{\alpha\alpha} - N_{\beta\alpha}$ and $N_{\alpha\beta} - N_{\beta\beta}$ are proportional to the thermal equilibrium Boltzman factor, $\Delta E_A/kT$, or simply ϵ_a. If it is assumed that the X transitions of the AX system are saturated by irradiation with $\mathbf{H}_2$ at about the X resonance frequency, then $N_{\alpha\alpha} = N_{\alpha\beta}$ and $N_{\beta\alpha} = N_{\beta\beta}$. If the relaxation mechanism p_2 predominates, then $N_{\alpha\alpha} - N_{\beta\alpha}$ and $N_{\alpha\beta} - N_{\beta\beta}$ will be proportional to the Boltzman factor $\epsilon_x + \epsilon_a$. If the Overhauser enhancement factor is defined as $(a - a_0)/a_0$ where a_0 = signal intensity without double resonance and a = signal intensity with double resonance, then the enhancement factor for the above example is simply ϵ_x/ϵ_a. If p_0 is the predominant relaxation mechanism, then the enhancement factor is $-\epsilon_x/\epsilon_a$. Thus, if $|\epsilon_x| > |\epsilon_a|$, the resonance will be inverted.

If the magnetogyric ratio of nucleus A is positive, while that of X is negative, then the energy level diagram appears as in Figure 4. For this case, if p_2 predominates, then the enhancement factor is $-\epsilon_x/\epsilon_a$, while if p_0 predominates, the enhancement factor is ϵ_x/ϵ_a.

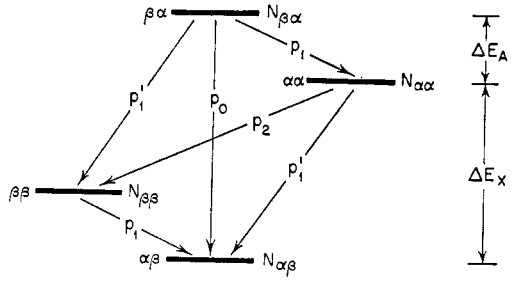

Fig. 4.—Energy level diagram for an AX system where the magnetogyric ratio of A is positive and the magnetogyric ratio of B is negative, and spin–spin coupling is neglected.

A time-dependent interaction of the type $\mathbf{I}(a)\cdot\mathbf{I}(x)$ contributes to p_0. A rapid exchange of nuclei that interact by the indirect coupling mechanism can thus lead to a large value of p_0. In the limit of very large p_0, the enhancement factor is $-\epsilon_x/\epsilon_a$ if the magnetogyric ratios are of the same sign, or ϵ_x/ϵ_a if the magnetogyric ratios are of opposite sign. The largest transition probability arising from the usual dipole–dipole relaxation mechanism is p_2, if the spectral intensities of the Brownian motion of the molecule in a liquid are assumed to be independent of frequency. However, since other transition probabilities compete with p_2 for the dipole–dipole mechanism, the enhancement factor is only $1/2\ \epsilon_x/\epsilon_a$ if the magnetogyric ratios are of the same sign, or $-1/2\ \epsilon_x/\epsilon_a$ if the magnetogyric ratios are of opposite sign.

Steady-state nuclear Overhauser effects for the HF system exhibiting all these features have been observed by Solomon and Bloembergen (98). The enhancement of the C^{13} resonances in $C^{13}-\{H^1\}$ experiments has been reported by Lauterbur (50).

C. DENSITY MATRIX TREATMENT

In the previous calculations, the assumption that the relative intensities are proportional to

$$|\langle\psi_{R_i}|\sum_i v_{1i}I_x(i)|\psi_{R_i}\rangle|^2$$

was made without justification, and relaxation mechanisms were disregarded. Complete treatments of the double resonance problem using the density matrix formalism have been given by Bloch (20) and Tomita (101). As in the work of Wangness and Bloch (104), Bloch (20) assumes that the nuclear spin system is in contact with the molecular system or lattice that is in thermal equilibrium. The density matrix for the entire system then is described as the statistical average of the density matrix for the spin system over the lattice. Bloch (20) further assumes that the molecular system remains in thermal equilibrium, even though it is coupled to the nuclear spin system which deviates from thermal equilibrium because of the application of $\mathbf{H}_2$. The time dependence of the density matrix arising from $\mathbf{H}_2$ is removed by a transformation to a rotating coördinate system analogous to equation (6). The nuclear induction signal then is calculated from the transformed density matrix for the spin system.

Abragam (4) has shown from a detailed theory of double resonance that the line intensity is in fact proportional to

$$|\langle\psi_{R_j}|\sum_i v_{1i}I_x(i)|\psi_{R_i}\rangle|^2$$

if relaxation effects are neglected. The intensities of the additional negative signals that appear when ω_1 is close to ω_2 also can be calculated readily from the density matrix treatment. If the density matrix for a spin system in the rotating coördinate system is given as the sum of a constant matrix ρ and a time dependent matrix χ, then the equation obeyed by χ is

$$\frac{d\chi}{dt} + i[\mathcal{H}_R^0,\chi] + i[\mathcal{H}_R'(t),\chi] + \Gamma(\chi) = -i[\mathcal{H}_R,\rho] \quad (48)$$

where $\Gamma(\chi)$ is a function that depends upon the relaxation Hamiltonian.

A solution of equation (48) of the form

$$<\psi_{R_i}|\chi|\psi_{R_j}> = z_{ij}e^{i\omega' t} \tag{49}$$

where $\omega'/2\pi = E_{R_j} - E_{R_i}$ can be obtained by taking the $<\psi_{R_i}|\ |\psi_{R_j}>$ matrix element of each term in equation (48). Following the notation of Abragam (4), the signal intensities are then proportional to terms of the type

$$|<\psi_{R_i}|\sum_i v_{1i}I_-(i)|\psi_{R_i}>|^2(\rho_i - \rho_j)$$

where $(\rho_i - \rho_j)$ is the difference between diagonal elements of the constant matrix ρ.

A solution to equation (48) of the form

$$<\psi_{R_j}|\chi|\psi_{R_i}> = z_{ji}e^{-i\omega' t} \tag{50}$$

is also possible. In this case, the signal is proportional to:

$$<\psi_{R_i}|\sum_i v_{1i}I_-(i)|\psi_{R_j}>|^2(\rho_j - \rho_i)$$

Thus if $\omega' \ll \omega_2$, two signals corresponding to the i→j transition will be observed in the laboratory system at frequencies $\omega_1/2\pi = (\omega_2 \pm \omega')/2\pi$. Since the sign of the term $(\rho_i - \rho_j)$ is different for the two solutions of equation (48), the intensity of the signal at $\omega_1/2\pi = (\omega_2 + \omega')/2\pi$ will be opposite in sign to the signal at $\omega_1/2\pi = (\omega_2 - \omega')/2\pi$. The relative intensity of these two signals depends on the relative magnitude of the matrix elements $|<\psi_{R_i}|\sum_i v_{1i}\ I_-(i)|\psi_{R_j}>|^2$ and $|<\psi_{R_j}|\sum_i v_{1i}\ I_-(i)|\psi_{R_i}>|^2$. These matrix elements will in general be different depending on the detailed form of ψ_{R_i} and ψ_{R_j}.

III. General Applications

A. Effects in the Limit of Large Amplitudes of $\mathbf{H}_2$

1. Spin Decoupling

Nuclear magnetic double resonance has had widest application as a spin-decoupling technique (8, 84, 93, 63). In the limit of large amplitudes of v_{2x}, the spectrum of a nucleus A that is coupled to a second nucleus X appears as a single line, rather than a multiplet. Although the effect of double resonance appears to be analogous to the effects of short relaxation times or chemical exchange in collapsing spin multiplets (71) these phenomena have quite different origins. The spectra observed for intermediate values of $\mathbf{H}_2$ (22, 14, 33) are quite different from those observed when the rate of reorientation of nucleus X by relaxation or chemical exchange is comparable to J (71). The elementary theory given in Section II shows that for large v_{2x}, the X nucleus is essentially quantized along the x direction, while the A nucleus is quantized in the z direction. Hence the term $J\mathbf{I}(a)\cdot\mathbf{I}(x)$ vanishes to first order, resulting in the collapse of the spin multiplet (74).

The description of the double resonance effect as arising from the saturation of the resonance of the X nucleus is improper (2). The condition for decoupling is $v_{2x} > J_{ax}$ (assuming A_x equals zero) which is quite different from the condition for saturation of the X nucleus, $\gamma_x^2H_2^2(T_1T_2)_x \gg 1$.

The relationship between saturation, "nuclear stirring," and decoupling can be given approximately as follows (50). For intermediate decoupling in an AX system

$$J_{ax} \sim v_{2x} \tag{51}$$

The minimum saturation of the X nucleus will occur for the shortest $(T_1)_x$ of interest, that which just allows the coupling to be resolved. This condition is

$$2\pi J_{ax} = 1/(T_1)_x \tag{52}$$

The saturation parameter, S_0, is given by (67)

$$S_0 = \frac{1}{1 + v_{2x}^2(T_1)_x(T_2)_x} \tag{53}$$

Assuming $(T_1)_x = (T_2)_x$, and using equations (51), (52), and (53)

$$S_0 = \frac{1}{1 + 1/4\pi^2} \tag{54}$$

Some saturation of nucleus X therefore accompanies decoupling in most cases of interest. However, saturation of nucleus X is only a side effect in the decoupling process.

For nucleus X of spin 1/2, the probability for transitions induced by $\mathbf{H}_2$ at exact resonance is (67)

$$P_x = 1/2\ v_{2x}^2(T_2)_x \tag{55}$$

From equations (51) and (52), and the assumption that $(T_1)_x \sim (T_2)_x$

$$P_x = 1/4\pi J_{ax} \tag{56}$$

Thus the transition rate, P_x, is considerably less than the rate usually assumed necessary for the collapse of a spin multiplet, $P_x \sim 2\pi J_{ax}$. Again, the change in P_x due to $\mathbf{H}_2$ is only a side effect in the decoupling process.

Complex spectra can be simplified by changing selectively the relaxation times of certain nuclei in a coupled spin system. This can be done, for example, with paramagnetic ions in proper concentration. This technique has been used with particular success for the examination of the B^{11} spectra of the boron hydrides (54). The collapse of spin multiplets by the selective variation of relaxation times is appropriately described as "nuclear stirring."

Spin decoupling is used in the analysis of spectra to remove complicating effects of certain nuclei, and to establish the correct assignment of spin–spin couplings. For nuclei with spin greater than 1/2, the possibility of

relaxation through the interaction of the nuclear quadrupole moment with the electric field gradient at the nucleus often leads to very small values of T_1. Spin multiplets arising from interaction with the high-spin nucleus are thus broadened. Decoupling the high-spin nucleus removes the complications arising from broadened spin-spin multiplets. Double resonance has been used to effectively decouple nuclei such as D^2, N^{14}, B^{10}, B^{11}, and Al^{27} as an aid in the analysis of proton resonance spectra (63, 93, 10, 65, 81, 62, 83).

Double resonance methods are also applicable in the analysis of spectra for which the overlap of complex multiplet patterns causes ambiguities in assignment that cannot be removed by computation. The proton spectrum of the $-CH_2CH_2-$ group of $[CF_3CH_2CH_2SiOCH_3]_3$ for example is reduced to a very tractable A_2B_2 case when the fluorine nuclei are decoupled (50). Freeman (29) has illustrated the analysis of propionaldehyde when the aldehydic protons are decoupled.

The correct assignment of spin–spin couplings can be established by selectively decoupling given nuclei, and noting the collapse of other spin multiplets. This technique has been applied to nuclei with very different magnetogyric ratios. The structure in the proton spectrum of B_5H_9 arising from coupling with the different boron nuclei was assigned by selectively decoupling the two different types of boron nuclei (93). The assignment of the fine structure in 1-methyl-2-pyridone by proton–proton decoupling has been illustrated by Turner (102).

2. *The Measurement of Chemical Shifts by Double Resonance*

Double resonance methods can be used to measure the Larmor frequency of a nucleus when an oscillator for detecting the resonance of this nucleus is not available (48). This technique was first used by Royden (84) to measure the C^{13} resonance frequency in $C^{13}H_3I$. The double resonance method is particularly useful for measuring chemical shifts of nuclei with small magnetogyric ratios, where the signal to noise ratio in most detectors is very low (11). As can be seen from the theoretical development in Section II, the double resonance effect does not depend on the existence of a population difference between the energy levels of the nucleus being studied. The nucleus being studied by double resonance, however, must be coupled to another nucleus that is easy to detect by the usual methods.

The double resonance method was used by Anderson, Pipkin, and Baird (7) in the determination of the relative magnetogyric ratios of N^{14} and N^{15}. It has also been shown (14) that by complete analysis of the intermediate spin-decoupling case, the resonance frequencies of N^{14} and N^{15} in NH_4^+ can be found to within $\pm$ 0.2 c./s. The sensitivity and accuracy of the measurement of chemical shifts by double resonance depends upon the details of the coupling, and the relaxation time of the nucleus whose shift is being measured. Thus, the N^{14} chemical shift in pyridinium ion can be measured to only $\pm$ 1 p.p.m. by decoupling the N^{14} from the acid proton, and the N^{14} chemical shift in pyridine can be measured to only $\pm$ 10 p.p.m. by decoupling the N^{14} from the α-protons (81).

It is also possible to use double resonance methods to measure the chemical shifts of protons that are obscured by overlapping features either from other protons in the same molecule, or by solvent resonances (102, 26). The proton that is obscured must be coupled to other protons whose resonances are observable. Turner (102) has used the double resonance technique to measure the chemical shifts of "hidden protons."

Freeman (30, 33) and Baldeschwieler (14) have noted that for the most accurate measurements of chemical shifts by double resonance, ν_{2i} should be small, of the order of J, and the spectrum should be obtained by sweeping the magnetic field. The value of the chemical shift must then be obtained by analysis of the double resonance spectrum. The measurement of proton chemical shifts in dichloroacetaldehyde by double resonance has been reported by Freeman (33) (see Figure 1). The accurate measurement of the N^{14} chemical shift in NH_4^+ is illustrated in Figure 5 (14).

B. EFFECTS FOR INTERMEDIATE AMPLITUDES OF $\mathbf{H}_2$

1. *Determination of the Amplitude of* $\mathbf{H}_2$

The determination of the amplitude of $\mathbf{H}_2$ by observing the double resonance spectrum of a single nucleus was first suggested by Bloch (20). Anderson (8) applied the technique using the proton spins of water. From equation (47), there are two values of ν_{0a} for which resonance occurs. These are given by

$$\nu_{0a}^{\pm} = \omega_2/2\pi \pm [((\omega_1 - \omega_2)/2\pi)^2 - \nu_{2a}^2]^{1/2} \qquad (57)$$

If $D^2 = (\nu_{0a}^+ - \nu_{0a}^-)^2$ is plotted against $((\omega_1 - \omega_2)/2\pi)^2$, a straight line results that intersects the axis of $((\omega_1 - \omega_2)/2\pi)^2$ at $((\omega_1 - \omega_2)/2\pi)^2 = \nu_{2a}^2 = \gamma^2 H_2^2/4\pi^2$ (8). Thus $\mathbf{H}_2$ can be determined precisely.

The amplitude of $\mathbf{H}_2$ also can be found by a complete analysis of the spectrum for the case of intermediate decoupling of two nuclei (14). The determination of H_2 from the $H-\{N^{15}\}$ double resonance spectrum of $N^{15}H_4^+$ has been given by Baldeschwieler (14). The observed and calculated spectra of $N^{15}H_4^+$ for various values of H_2 are shown in Figure 6.

2. *Effects of Sweeping Magnetic Field*

From equations (20) and (39) it is seen that sweeping the magnetic field while ω_1 and ω_2 remain constant introduces considerable complication into the double resonance spectrum. The terms γ_x/γ_a in equation (39) cause almost a doubling of the number of separate

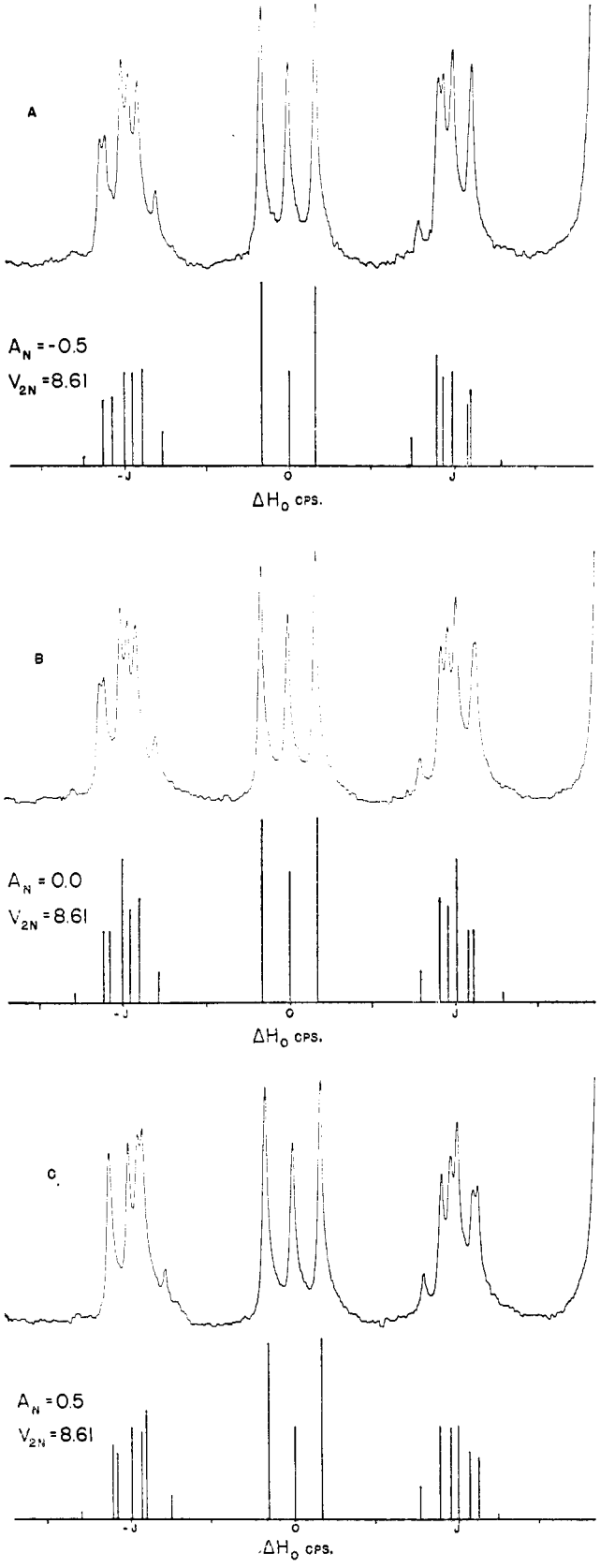

Fig. 5.—Double resonance spectra of $N^{14}H_4^+$ at 40.0 Mc./s. obtained by the field-sweep method where ν_{2N} = 8.61 c./s., and (a) A_N = −0.5 c.s., (b) A_N = 0.0 c./s., and (c) A_N = 0.5 c./s. (14).

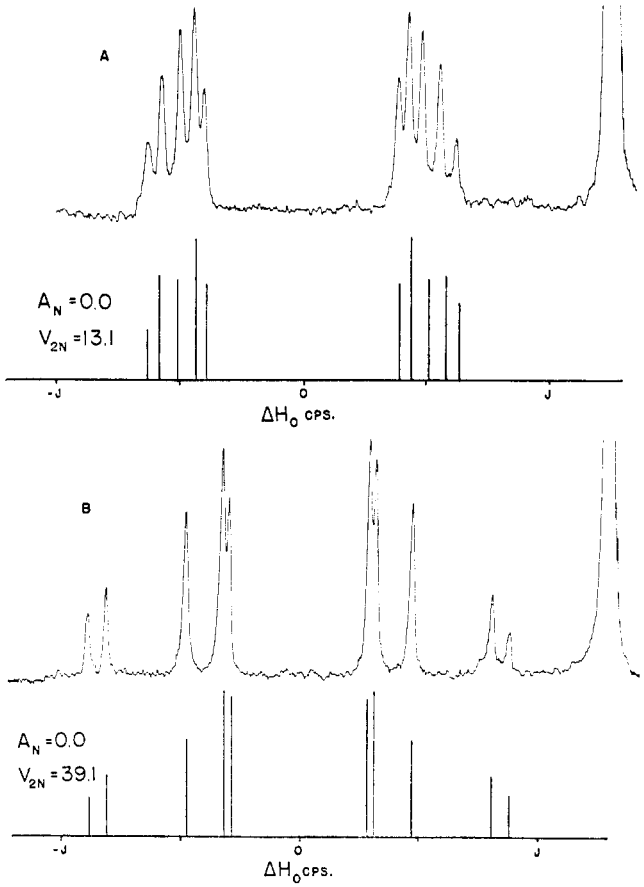

Fig. 6.—Double resonance spectra of $N^{15}H_4^+$ at 40.0 Mc./s. obtained by the field-sweep method where A_N = 0.0 c./s. and (a) ν_{2N} = 13.1 c./s., and (b) ν_{2N} = 39.1 c./s. (14).

lines observed in the spectrum of an A_nX molecule. Furthermore, when A_x is not equal to zero, the spectrum for an A_nX molecule loses its symmetry about ΔH_0 equal to zero (14). The change in symmetry with change in A_x, or equivalently in ω_2, provides a very precise technique for finding ν_{ox} (14). The frequency ω_2 for which A_x equals zero thus can be found quickly from the qualitative shape of the spectrum without resorting to detailed calculation. When a value of ω_2 has been located which gives a symmetric spectrum, the procedure can be checked by recording the spectra at several c./s. on each side of $\omega_2/2\pi = \nu_{ox}$. These spectra will be mirror images for an A_nX system if $\omega_2/2\pi = \nu_{ox}$ (14). Double resonance spectra of $N^{14}H_4^+$ where A_n equals −0.5, 0.0 and +0.5 c./s. are shown in Figure 5.

The effects of sweeping H_0 and ω_1 are illustrated for an AX system in Figure 1. From the spectra for a frequency-sweep experiment it is apparent that a small difference of A_x from zero can only be recognized as a small splitting of the central line. The loss of symmetry and splitting of the central feature in a field sweep experiment are apparent for smaller differences of A_x from zero. Thus chemical shifts can be measured more accurately by the field-sweep technique. As can be seen from equation (19), for large values of ν_{2x}

the difference between the double resonance spectra observed by the two methods disappears.

There are, however, situations when the frequency-sweep method has obvious advantages over the field-sweep technique. If the spectrum of an A nucleus extends over a large frequency range, then only with a frequency-sweep technique is it possible to observe all of the A spectrum in decoupled form. When an AB system is examined by double resonance, the interpretation of the field-sweep experiment becomes very complicated.

The special effects of sweeping magnetic field rather than frequency are most pronounced when $\omega_2 \gg \omega_1$. For these cases, the ratio γ_x/γ_a is larger than one, and equation (39) must be solved directly for ΔH_0. The C^{13}–$\{F^{19}\}$ double resonance of CF_3COOH is a striking example of the effects of sweeping magnetic field where $\gamma_{F^{19}}/\gamma_{C^{13}} = 3.75$ (50). The two C^{13} resonances in CF_3COOH differ by 63 ppm. (49). Hence, with $\omega_1/2\pi$ equal to 8.5 Mc./s., $(\omega_2' - \omega_2)/2\pi$ is equal to 2010 c./s., where $\omega_2'/2\pi$ is the frequency required to decouple the F^{19} from the C^{13} of the carboxyl group, and $\omega_2/2\pi$ is the frequency required to decouple the F^{19} from the C^{13} of the CF_3 group. Although the fluorines are equivalent, $(\omega_2' - \omega_2)/2\pi$ equals 2010 c./s. and the fluorines must be separately decoupled from the carbons of the CF_3 and COOH groups. Depending on the ratio γ_x/γ_a, the sweep rate, and the relaxation times for the various nuclei, the effects of rapid passage conditions on the signal shape may require consideration.

From the effects of sweeping magnetic field, it is possible to determine whether $|\omega_2/2\pi|$ is larger or smaller than $|\nu_{ox}|$ (14). The double resonance spectrum, however, is invariant with change in sign of γ_x as well as with change in sign of J (13). Thus no information on the absolute signs of magnetogyric ratios or coupling constants can be obtained by this technique. Shimizu and Fujiwara (92), however, have suggested that the absolute signs of coupling constants can be obtained from multiple resonance spectra if the complete density matrix formulation including relaxation effects is considered.

3. *Relative Signs of Coupling Constants*

Although the absolute signs of coupling constants cannot be found by double resonance when relaxation effects are neglected, information on the relative signs of coupling constants can be obtained. When at least three non-equivalent protons are coupled together, the relative signs of the coupling constants can be found from a double resonance experiment, even though the spectrum is first order (32, 56). The relative signs of the coupling constants in systems of at least three non-equivalent nuclei can be obtained by the analysis of the usual n.m.r. spectrum of the system only when the spectrum contains second-order features (23).

The determination of the relative signs of the coupling constants in a first order AMX spectrum by double resonance has been given by Freeman (32). The spin states of the three nuclei of spin 1/2 in an AMX system corresponding to the theoretical twelve line spectrum are shown in Table VI. For this example it is assumed that all the coupling constants have the same sign.

TABLE VI

SPIN STATES OF NEIGHBORING NUCLEI FOR AMX SYSTEM WITH THE SIGNS OF ALL COUPLING CONSTANTS THE SAME

Origin of transition		X				A				M			
Transition no.		12	11	10	9	8	7	6	5	4	3	2	1
Spin states of neighboring nuclei	A	α	β	α	β					α	α	β	β
	M	α	α	β	β	α	α	β	β				
	X					α	β	α	β	α	β	α	β

If it is possible to irradiate at a frequency $\omega_2/2\pi$ which is intermediate between the frequencies of the transitions 7 and 8, and if $\nu_{2a} > J_{ax}$, lines 11 and 12 should coalesce, while lines 9 and 10 should be unaffected. This process is equivalent to decoupling the A and X nuclei only in those molecules that have nucleus M in state α. If J_{am} and J_{mx} were of opposite sign, the α's and β's in row M of column X or column A should be interchanged. Irradiation with $\omega_2/2\pi$ between lines 7 and 8 would cause the coalescence of lines 9 and 10, if J_{am} and J_{mx} were of opposite sign. The analogous experiment can be applied to find the relative signs of J_{am} and J_{ax}. If $\omega_2/2\pi$ lies between the frequencies of lines 1 and 2, then lines 9 and 11 should coalesce if J_{am} and J_{ax} have like signs. Lines 10 and 12 will coalesce, however, if J_{am} and J_{ax} are of opposite sign.

The success of this experiment depends on the possibility of obtaining a field $\mathbf{H}_2$ with $\omega_2/2\pi$ between transitions 7 and 8, for example, without perturbing transitions 5 and 6. Thus, $\nu_{2a} = \gamma_a H_2/2\pi$ must be of the order of J_{ax} so that spins A and X can be decoupled. Yet, $\nu_{2m} = \gamma_m H_2/2\pi$ must be small enough so that off-diagonal elements in ν_{2m} can be neglected in the matrix of the Hamiltonian for the AMX system. With decreasing relative chemical shift between nucleus A and M, increasing H_2, and increasing values of J_{am}, the off-diagonal elements in ν_{2m} and J_{am} become more significant. If these off-diagonal elements cannot be neglected, the double resonance spectrum becomes considerably more complex, as discussed for the AB case in Section II. In the limit that these off-diagonal elements can be neglected, the state of nucleus M can be considered as independent of the double resonance experiment between A and X, and the relative signs of J_{am} and

J_{mx} can be found easily. The determination of the relative signs of coupling constants in AMX systems has been illustrated by Freeman (30).

4. *Measurement of Small Relative Chemical Shifts*

Small relative chemical shifts should give rise to significant changes in the double resonance spectrum of a spin system. The double resonance technique should thus be useful for measuring chemical shifts and coupling constants in molecules where the nuclei are nearly equivalent. As shown in Section II, the double resonance spectrum is independent of the coupling constants between equivalent nuclei.

The changes in the A–$\{X\}$ double resonance spectrum calculated for a tetrahedral A_4X species (where A and X are of spin 1/2) with small changes in the chemical shift of one A nucleus are given in Figure 7 (14). In Figure 6b the double resonance spectrum of

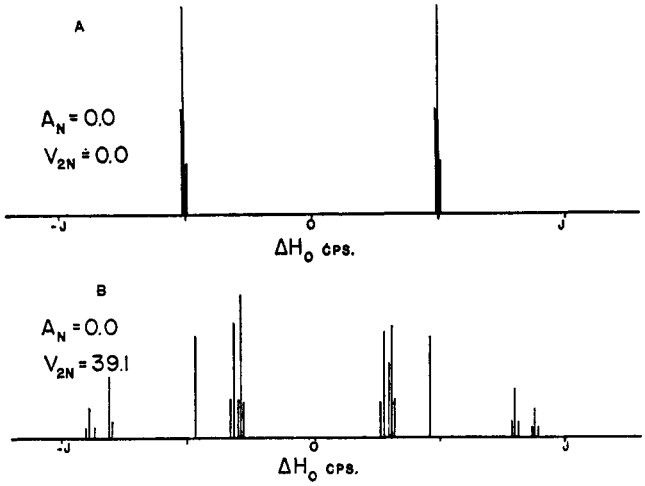

Fig. 7.—Calculated double resonance spectra for an $A_3A'X$ system where $J_{ax} = J_{a'x} = 73.7$ c./s., $J_{aa'} = 12.4$ c./s., $\delta_{a'a} = 2.0$ c./s., $A_x = 0.0$ c./s., and (a) $\nu_{2x} = 0.0$ c./s., and (b) $\nu_{2x} = 39.1$ c./s. (14).

an A_4X molecule is shown with $J_{ax} = 73.7$, $\nu_{2x} = 39.1$ and $A_x = 0.0$ c./s. The spectrum for a C_{3v} molecule, $A_3A'X$, with A′ 2 c./s. upfield from A, with $J_{aa'} = 12.4$, $J_{ax} = J_{a'x} = 73.7$, $\nu_{2x} = 39.1$ and $A_x = 0.0$ c./s. is shown in Figure 7b. The effect of a small change in the A' chemical shift on the double resonance spectrum is striking. The normal high-resolution n.m.r. spectrum calculated for the distorted species is shown in Figure 7a. The normal n.m.r. spectrum of the A nuclei of the undistorted molecule is simply a pair of lines separated by J_{ax}. The double resonance technique thus has potential application to the study of molecules where the resonances of nearly equivalent nuclei cannot be resolved by usual n.m.r. methods.

5. *Measurement of Relaxation Times and Exchange Rates*

The occurrence of a nuclear Overhauser effect depends on the relaxation mechanisms in a spin system. Both the relaxation times and exchange rates in HF have been determined from transient and steady-state Overhauser effects (98). The line widths and intensities depend in a complex way on the relaxation times of the various nuclei in a spin system as shown by Bloch (20).

For nuclei with spin greater than 1/2, the most important relaxation mechanisms may occur through interaction of the nuclear quadrupole moment with electric field gradients at the nucleus. The effects of quadrupole relaxation on the relative line widths of a double resonance spectrum have been calculated (12).

IV. INSTRUMENTATION

A. NUCLEI WITH VERY DIFFERENT MAGNETOGYRIC RATIOS

1. *Locked Oscillator System*

The second radio frequency field for H–$\{N^{15}\}$ double resonance has been supplied with a locked oscillator system (14). A block diagram of the system is shown in Figure 8. The output of a General Radio 1211-B

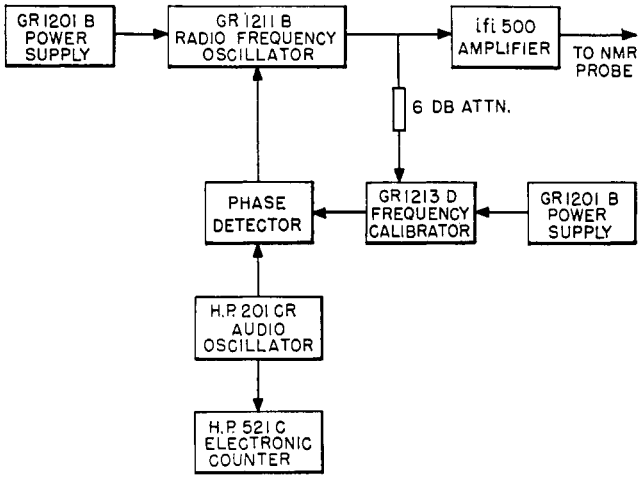

Fig. 8.—Locked oscillator system for decoupling nuclei with very different magnetogyric ratios.

Unit Oscillator is mixed with one of the 10 kc. harmonics of a General Radio 1213-D Unit Time/Frequency Calibrator. The audio-frequency beat signal from the calibrator is mixed in a phase detector with the output of an audio oscillator. The output of the phase detector then is returned to the grid of the 5763 tube in the 1211-B Unit Oscillator. The stability of the system then depends on the stability of the audio oscillator, and on the stability of the frequency standard. With this system, considerable care is necessary to avoid the introduction of unwanted harmonics into the radio-frequency output.

2. *Audio-frequency Modulated Crystal Oscillator*

A very stable radio-frequency field that is variable over several kilocycles per second can be supplied by an audio-modulated crystal oscillator (14). If a balanced modulation scheme is used, only the two audio-frequency sidebands appear in the output of the oscillator. Either sideband then can be used as a second radio-frequency source. The audio-frequency modulated oscillator has the disadvantage that it is variable only over a range of several kilocycles per second. Crystal oscillators modulated with a variable radio-frequency oscillator have a wider frequency range, but are limited in stability by the stability of the variable frequency oscillator.

3. *Audio-frequency Modulated Frequency Divider*

Glassel, Turner and Jackman (34) have used a 56.4 Mc. oscillator and a frequency divider to produce a radio-frequency signal close to the N^{14} resonance frequency. A final audio-frequency modulation permits the adjustment of the decoupling frequency to the exact N^{14} resonance frequency.

B. NUCLEI WITH NEARLY EQUAL MAGNETOGYRIC RATIOS

1. *Locked Oscillator System*

The decoupling of chemically non-equivalent protons using a locked oscillator system was first demonstrated by Anderson (8). The frequency of one of two crystal oscillators was controlled by a variable reactance circuit. The frequency difference between the two oscillators was stabilized by mixing the outputs to obtain the difference frequency, which then was compared with the reference frequency from an audio oscillator in a phase-sensitive detector. The output voltage of the phase detector was in turn used to control the variable reactance.

2. *Field and Frequency Modulation*

Itoh and Sato (40) have shown that proton–proton decoupling is possible with considerably simplified instrumentation. The fixed frequency radio-frequency oscillator of the spectrometer is used as $\mathbf{H}_2$ rather than $\mathbf{H}_1$, and thus is set to high power, while the magnetic field is modulated at the frequency $\omega'/2\pi$. If an AX system is considered, and the fixed frequency of the spectrometer, $\omega_2/2\pi$, is equal to ν_{ox}, then when $\omega'/2\pi = \nu_{ox} - \nu_{oa}$, the spectrum of nucleus X and the sideband of the spectrum of nucleus A are superimposed in the output of the spectrometer. If the amplitude of $\omega'/2\pi$ is small enough so that the signal of the sideband can be recorded without saturation, and if $\nu_{2x} > J_{ax}$, decoupling of spins A and X can be observed.

With the sideband technique of Itoh and Sato (40), the desired sideband response is superimposed on the signal from nucleus X, which may be partially saturated, but not completely absent. A simple method of eliminating the unwanted signal is to use a lock-in detector as suggested by Pound (73) and Freeman and Pound (31). The lock-in detector is referenced to the modulating frequency, $\omega'/2\pi$. Various types of lock-in detectors for this purpose have been described by Freeman (29), Kaiser (42), Anderson and Johnson (9), and Elleman and Manatt (25). A schematic diagram of the lock-in detector used by Elleman and Manatt is shown in Figure 9.

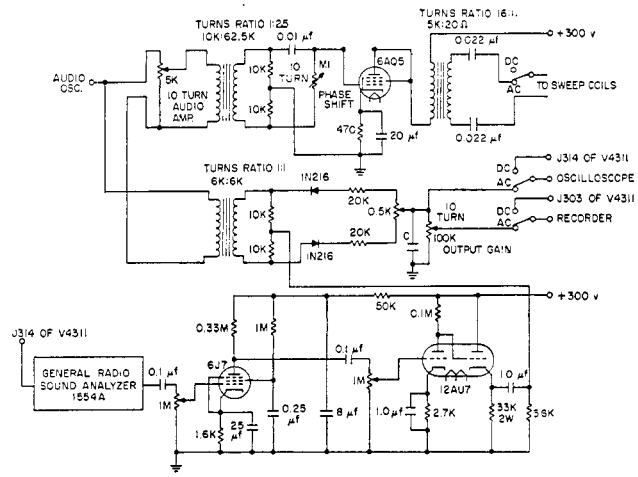

Fig. 9.—Lock-in-detector for decoupling nuclei with nearly equa magnetogyric ratios (25).

The magnetic field modulation schemes described above produce a symmetrical pair of sidebands at $\nu_{ox} \pm \omega'/2\pi$. The presence of a second sideband introduces no particular complication for simple spin systems. However, for more complicated spin systems, additional resonance lines appear due to the unwanted sideband, and the double resonance technique may hinder rather than aid in the analysis of the spectrum. Turner (102) has described a system using single side-band suppressed carrier modulation of the fixed frequency of the spectrometer. The fixed radio-frequency of the spectrometer becomes $\mathbf{H}_1$, and the single sideband is used as $\mathbf{H}_2$.

Effects arising from the unwanted sideband also can be eliminated by modulating the magnetic field at two frequencies, one to produce a weak sideband which is used as $\mathbf{H}_1$ and another to produce a stronger sideband which becomes $\mathbf{H}_2$ (33). In this way the modulation frequencies can be made quite large so that the center band and the two unused sidebands are kept far from the region of the spectrum, while the difference between the two audiofrequencies can remain small, of the order of the relative chemical shifts in the spectrum.

Freeman (33) has used modulation at two audio-frequencies, with two lock-in detectors to produce a frequency-sweep spectrometer system. For this appli-

cation, one of the audio-frequency sidebands is used with a lock-in detector to stabilize the magnetic field, following the procedure of Primas (77). The center-band is used as $\mathbf{H}_2$, and the other audio frequency side-band is used as a variable frequency field $\mathbf{H}_1$.

V. Specific Applications

The application of the general uses discussed in Section III to specific chemical problems will be treated in this section. The examples will be considered in the order governed by the atomic number of, firstly, the nucleus being studied with the weak field and, secondly, the nucleus being irradiated with the strong field.

A. $H^1-\{H^1\}$

The first examples of proton–proton decoupling were produced by Anderson(8). In the simple AX spectrum of dichloroacetaldehyde the doublet at lower field was made to coalesce by irradiation of the doublet at higher field. The more complicated ABX_2 system of 2,3-dibromopropene was reduced to a simple AB case by irradiation at the methylene resonance frequency.

Decoupling in acetaldehyde (A_3X spectrum) has been accomplished by a number of workers. Turner (102), using frequency modulation, obtained the value of 7.55 ± 0.02 p.p.m. for the chemical shift between the methyl and aldehyde protons, which compares favorably with the value of 7.59 ± 0.02 p.p.m. obtained by Manatt and Elleman (57), who used magnetic-field modulation (see Figure 10).

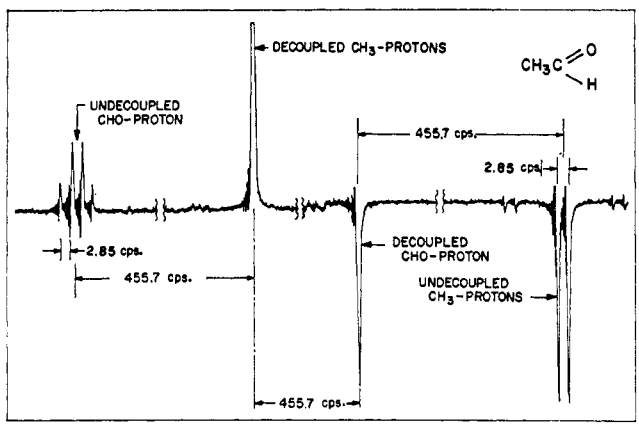

Fig. 10.—Single and double resonance spectra of acetaldehyde at 60 Mc./s. where ν_{2x} = 13.0 c./s. (57).

Turner also has illustrated the technique with ethanol (A_3M_2X spectrum) and has obtained the value 2.28 ± 0.02 p.p.m. for the chemical shift between the methyl and methylene protons (102).

Of more interest is the measurement of the chemical shift of protons which have their resonances obscured by other freatures in the spectrum, but which are spin-coupled to a nucleus whose resonance is observed. One example of the measurement of the chemical shift of such "hidden" protons is the study of the phenylhydrazine derivative of periodate-oxidized methyl 4,6-O-benzylidene-α-D-glucoside, for which the structure (I) was established (102).

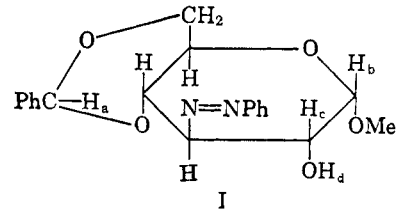

I

The spectrum (35) contains two resonances ascribable to the acetal protons H_a and H_b. The resonance at higher field can be assigned to H_b and exhibits a doublet splitting due to coupling to H_c. The position of the resonance due to H_c, which is in the middle of a complex, high-field band produced by the protons of the sugar ring, was located by $H^1-\{H^1\}$ double resonance (102). When H_d is replaced by an acetyl group, the H_c resonance is moved to lower field where it overlaps H_a. A further double resonance experiment confirms that it is spin coupled to H_b.

A second example of a "hidden" proton is H_a in the partial structure (II) of Clerodin. Its position was found by a double resonance experiment involving H_b to which it was spin coupled. The result confirmed the dihydrofuranoid nature of this portion of the Clerodin structure.

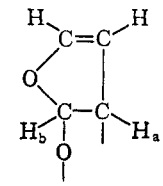

II

Frequently, a given type of proton produces a wide signal due to unresolved spin–spin splittings. The accurate determination of the chemical shift of such a group by the single resonance method then is difficult and the double resonance experiment is of advantage. Such an example is 1-methyl-2-pyridone (III) in which the H_4 and H_6 protons give broad signals which overlap. The shift between these groups has been found to be 12 c./s. by decoupling experiments involving the H_5 and H_3 protons (102).

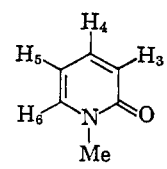

III

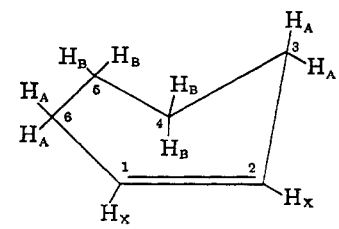

IV

In cyclohexene (IV) the α- and β-methylene resonances are each asymmetrical and about 20 c./s. wide. The chemical shift of the α-protons relative to the vinyl protons has been determined by double irradiation of the α-signal and observation of the vinyl resonances as shown in Figure 11 (57). The assignment of the spectrum was made on the basis that the α-proton group of lines should be the most complicated (58). When the double resonance experiment is repeated but with observation of the α-proton signal, not only is the α-methylene region considerably simplified but the resolution of the β-methylene region is improved as shown in Figure 12. This suggests that there is a long-range, unresolved coupling between the β- and vinyl protons (58). Similar studies of cyclopentene failed to reveal a long-range coupling (58).

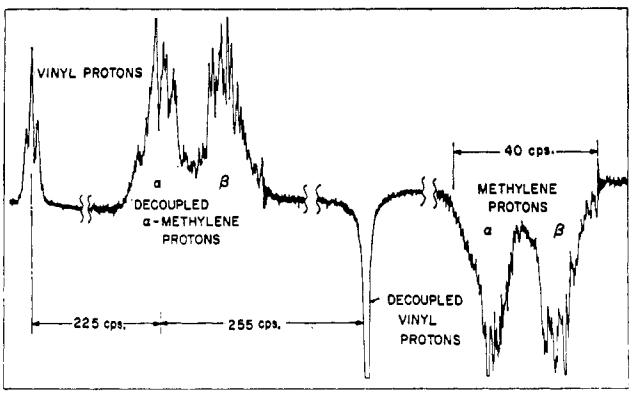

Fig. 11.—Single and double resonance spectra of cyclohexene at 60 Mc./s. where $\nu_{2x} = 20.0$ c./s. (57).

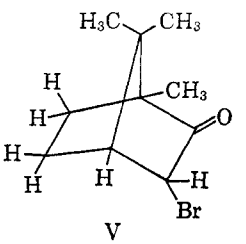

V

The assignment of the H_4 proton of α-bromocamphor (V) has been made by observation of the effects of decoupling it from the H_3 proton (see Figure 13) (57). The H_3 resonance is assigned to low field because of the expected effect of the carbonyl and bromine groups upon its chemical shift.

Assignments are sometimes difficult because two spin–spin coupling constants may be nearly equal. Two such examples are 3,6-anhydro-1,2-O-isopropylidene-5-O-tosyl-α-D-glucofuranose (VI) and 3,6-anhydro-1,2-O-isopropylidene-α-D-glucofuranose (VII) (6).

The protons H_2 and H_3 have similar shifts and each gives a doublet with a 3.5 c./s. splitting although J_{23} is too small to be observed (6). The signal from H_1 is also a doublet of 3.5 c./s. arising from coupling to H_2.

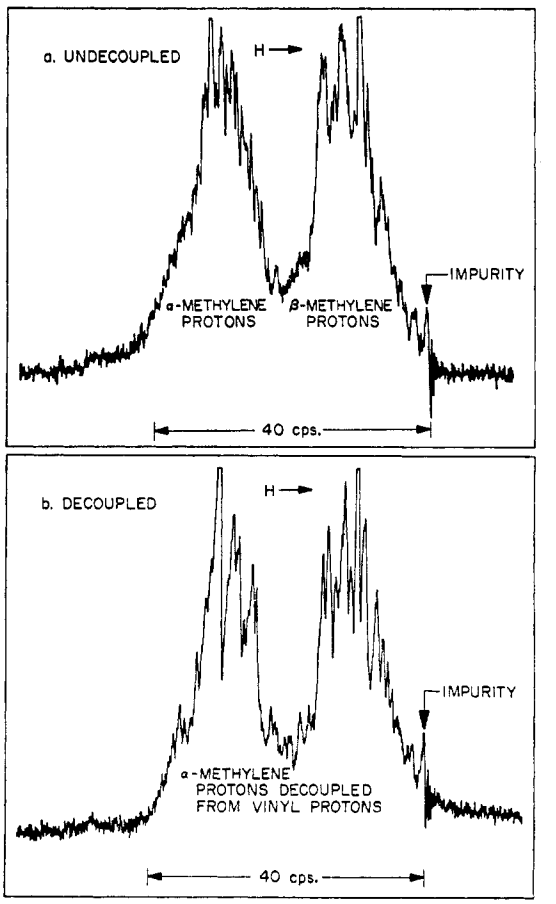

Fig. 12.—Spectra of methylene protons of cyclohexene at 60 Mc./s. where (a) the vinyl protons are undecoupled and (b) the vinyl protons are decoupled by the audio-frequency sideband technique (58).

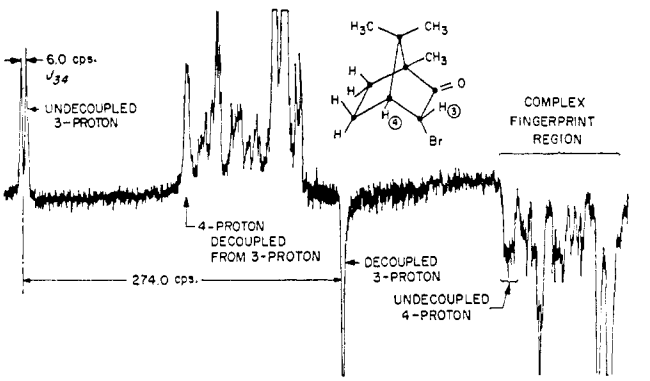

Fig. 13.—Single and double resonance spectra of α-bromocamphor at 60 Mc./s. where $\nu_{2x} = 6.0$ c./s. (57).

Thus the signal due to H_2 can be assigned by means of a double resonance experiment involving H_1. Double irradiation of H_3 did not affect the H_1 doublet.

The proton resonance spectrum at 60 Mc./s. of propionaldehyde has been analyzed completely with the aid of H^1–$\{H^1\}$ double resonance (29). The methyl-group resonance is typical of the A part of an ethyl group, A_3B_2. The aldehyde proton gives a simple triplet with a splitting of 1.3 ± 0.1 c./s. The molecule

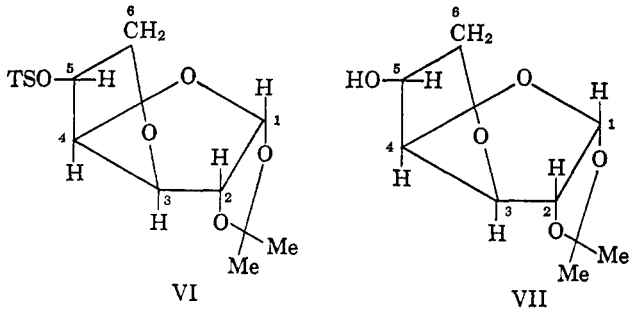

VI VII

is thus classed as an A_3B_2X case, where $J_{BX} = 1.3$ c./s. The methylene portion of the spectrum is shown in Figure 14a. Figure 14b shows the same region when

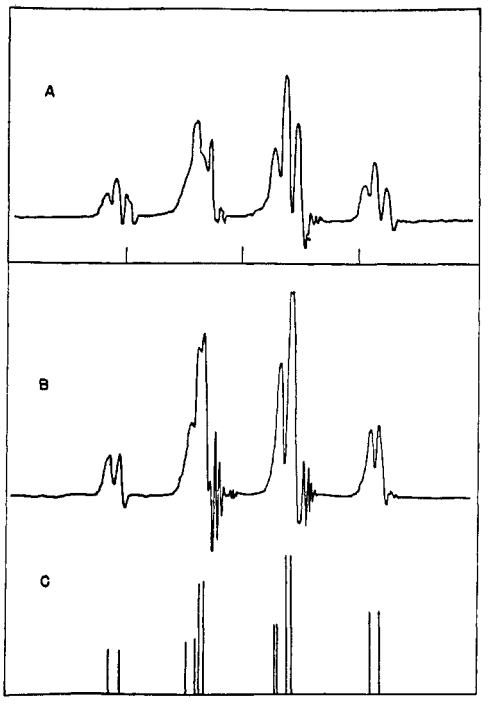

Fig. 14.—(a) Spectrum of CH_2 group in propionaldehyde with markers at 10 c./s. (b) The same spectral region with the aldehydic proton strongly irradiated. (c) Spectrum calculated with $J/\delta = 0.087$ and no coupling with the aldehydic proton (29).

the aldehyde group is strongly irradiated. The analysis is now simplified and the spectrum calculated with $J_{AB} = 7.4 \pm 0.1$ c./s. and $\delta_{AB} = 85.4 \pm 0.5$ c./s. is shown in Figure 14c.

The simplification of an $ABCX_3$ case to an ABC system by double irradiation is exemplified by the work of Manatt and Elleman on propylene oxide (60). The spectrum is dramatically simplified when the methyl, X_3, group is irradiated. The same authors have studied the proton resonance spectrum of cyclopentadiene at 60 Mc./s. (60). The $A_2B_2X_2$ spectrum is reduced to an A_2B_2 type by irradiation of the methylene protons.

The relative signs of coupling constants have been determined by double irradiation in a number of cases. The first of these was the diethylthallium cation, for which it was shown that the relative signs of the thallium–proton spin coupling constants were different for $J_{(Tl^{205}-CH_3)}$ and $J_{(Tl^{205}-CH_2)}$ (102, 56).

Similar experiments for cases where the three spins involved are all protons have been performed. Freeman and Whiffen (32) studied the four-spin system 2-furoic acid (VIII). The acid proton does not couple

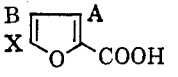

VIII

into the ring and hence only the ABX part of the spectrum is considered (see Figure 15). The treatment is

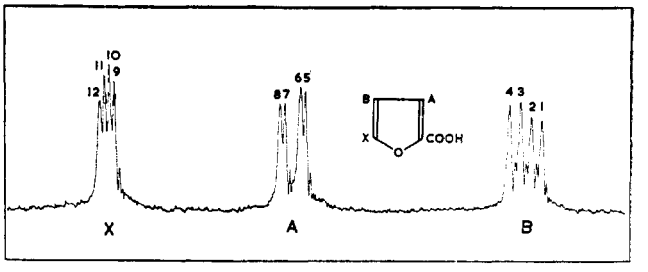

Fig. 15.—The A, B, and X parts of the spectrum of 2-furoic acid at 60 Mc./s. (32).

then as given in Section III-B-3. The appearance of the X region when various other transitions are irradiated is shown in Figure 16. It can be deduced from

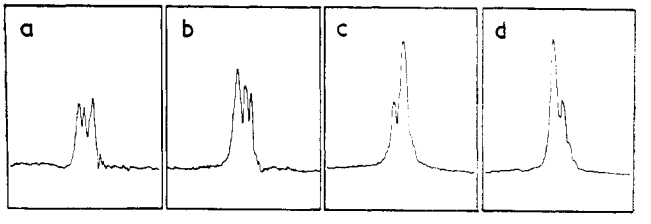

Fig. 16.—The X spectrum of 2-furoic acid at 60 Mc./s. with simultaneous strong irradiation of (a) transitions 5 and 6, (b) 7 and 8, (c) 1 and 2, (d) 3 and 4 (32).

the decoupled spectra that the signs of the three coupling constants between the ring protons are all the same.

The protons of the five-membered ring of indene (IX)

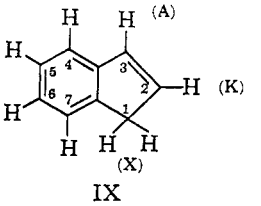

IX

have been treated similarly (25). They constitute an AKX_2 case. The 60 Mc./s. spectrum is shown in Figure 17. It is assigned as shown on the basis of the chemical shifts. The values derived for the coupling constants are: $J_{AK} = 5.58$ c./s.; $J_{AX} = 1.93$ c./s.; and $J_{KX} = 1.98$ c./s.

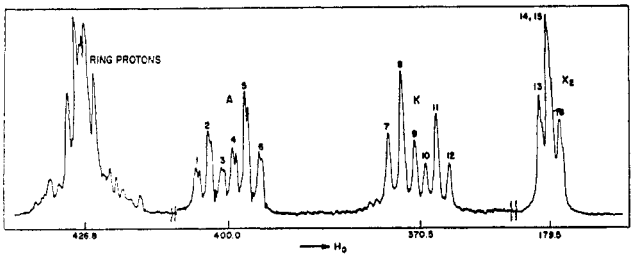

Fig. 17.—The spectrum of indene at 60 Mc./s.: the A and K regions were recorded at twice the gain used for the aromatic ring proton and X_2 regions (25).

The predicted spectra of the X_2 region for various relative signs and for the irradiation of various transitions are shown in Figure 18. The actual spectra obtained are shown in Figure 19, and it is clear that the

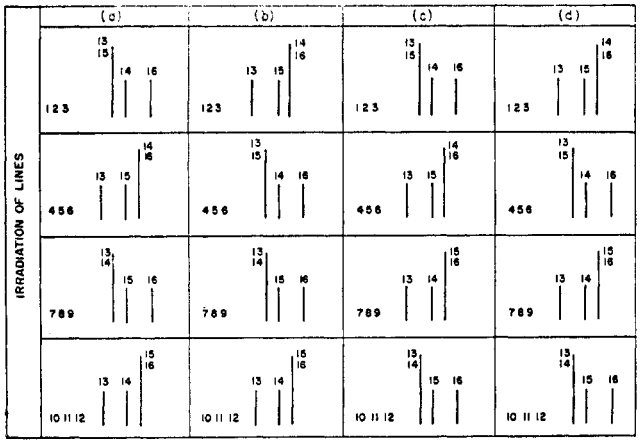

Fig. 18.—Calculated spectra for the X_2 region of indene for various relative sign assignments: (a) all J_{ij}'s of the same sign, (b) J_{kx} opposite in sign from J_{ak} and J_{ax}, (c) J_{ax} opposite in sign from J_{ak} and J_{kx}, (d) J_{ak} opposite in sign from J_{ax} and J_{kx} (25).

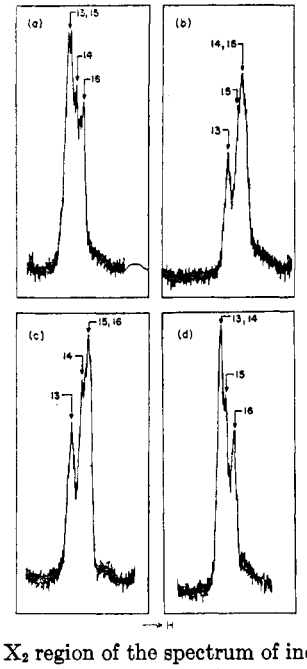

Fig. 19.—The X_2 region of the spectrum of indene at 60 Mc./s. with (a) lines 1, 2, 3 irradiated, (b) lines 4, 5, 6 irradiated, (c) lines 7, 8, 9 irradiated, (d) lines 10, 11, 12 irradiated (25).

sign of J_{AX} is different from the signs of J_{AK} and J_{KX}, *i.e.*, column c of Figure 18 obtains. This is consistent with the absolute sign assignment made using the theory of Karplus (43, 44) from which it is predicted that J_{AX} should be negative, and both J_{AK} and J_{KX} should be positive (25).

An additional splitting of 0.5 c./s. was observed in the A region and presumably is caused by H_4. Additional structure on the X_2 spectrum may also be seen in Figure 20b. The additional splitting is caused by long-range coupling with protons in the aromatic ring, as proven by the double irradiation spectrum shown in Figure 20a.

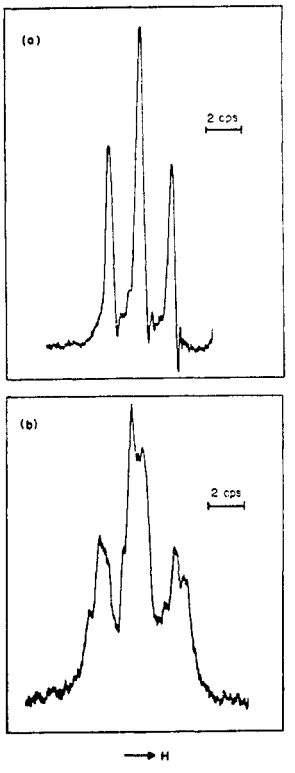

Fig. 20.—The X_2 region of the spectrum of indene at 60 Mc./s. with (a) double irradiation of the aromatic ring protons and (b) normal spectrum of X_2 region at a slightly lower sweep rate (25).

The applicability of the double resonance method for the determination of relative signs of coupling constants from spectra which show second-order effects has been considered (30, 59).

Freeman has studied the molecules *trans*-crotonaldehyde (X) and *trans*-crotonic acid.

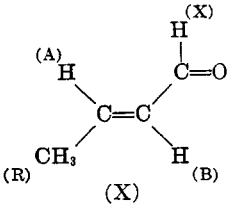

In the latter the acid proton was found to undergo exchange and it was not spin-coupled to the other protons of the molecule. In the aldehyde J_{AX} and J_{RX} are both zero, and the only splitting of the X region is due to J_{BX}. Consequently, the sign of J_{BX} relative to the signs of other coupling constants in the molecule could not be found.

The relative sign of J_{AB} and J_{BR} is found by observation of the A region and irradiation of transitions in the R region. Figure 21 shows the whole of the proton spectrum taken at 60 Mc./s. Figure 22a shows the decoupling of the high-field, A, quartet when the irradiation frequency is set at y, *i.e.*, is intermediate between transitions 1 and 3. Figure 22b shows the decoupling of the low-field A quartet when irradiation at z is used. The signs of J_{AB} and J_{BR} are different.

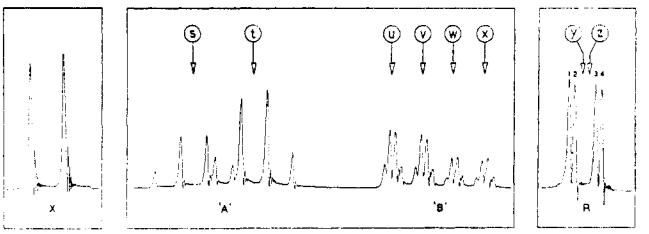

Fig. 21.—The spectrum of neat *trans*-crotonaldehyde at 60 Mc./s.: the arrows indicate the location of the strong field H_2 in the double resonance experiments (30).

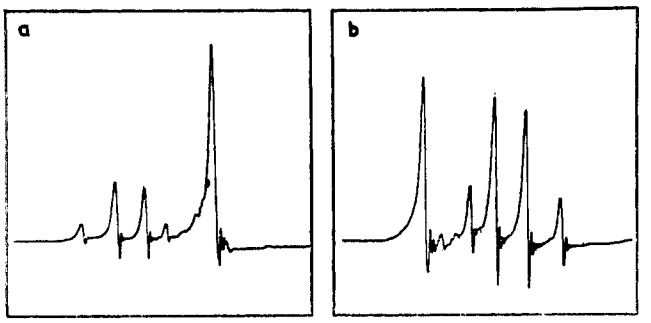

Fig. 22.—The A spectrum of *trans*-crotonaldehyde at 60 Mc./s. recorded with simultaneous irradiation of the R group with H_2 = 2.6 milligauss (a) at position (y), and (b) at position (z) as shown in Figure 21 (30).

Freeman points out that y and z differ by only 1.4 c./s., so that H_2 must be kept as low as possible compatible with efficient decoupling of A and R to avoid the collapse of both the A quartets. It is also important to take into account the fact that the separation of sideband and centerband is not exactly equal to the modulation frequency, as discussed in Section II-A-4.

Freeman (30) found that it was not possible to determine the relative signs of J_{AB} and J_{BR} by irradiating in the A region. The reason is that $J_{AR} > J_{BR}$ so that the large values of H_2 required to decouple the A and R spins affect the B region as well. Since transitions in this region are "mixed" transitions and do in fact involve the A spin, some decoupling between B and R occurs.

It is, however, possible to irradiate in the B region and to observe the R resonance without decoupling the A and R spins. Lower power levels are sufficient in this case because of the relatively small value of J_{BR}. J_{AB} and J_{AR} were found to have like signs in this way. The X spin produces a slight complication in that decoupling occurs for only half the molecules present, *i.e.*, for those in a given spin-state of X. Figure 23a

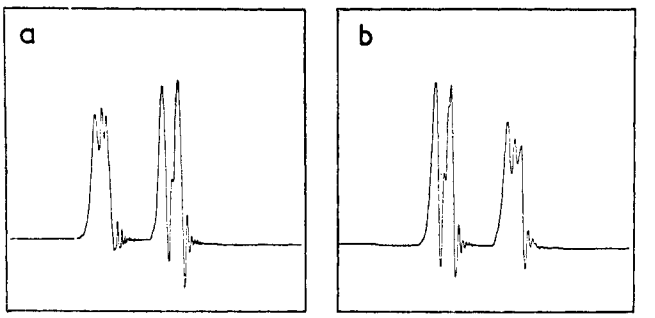

Fig. 23.—The R spectrum of *trans*-crotonaldehyde at 60 Mc./s. recorded with simultaneous irradiation of the B region with H_2 = 0.4 milligauss (a) at position (u), and (b) at position (k) as shown in Figure 21 (30).

shows the R spectrum when irradiation at either u or v is used. Figure 23b is the case where the irradiation frequency is either at w or x. Complications of this sort may limit the use of double resonance determinations of the relative signs of coupling constants in cases where the number of coupling constants is five or more.

This double resonance work on *trans*-crotonaldehyde and *trans*-crotonic acid confirmed the relative signs which had been deduced earlier from "second-order" spectra taken at frequencies below 60 Mc./s. (47, 66).

A second double resonance study of a spin-system containing an AB grouping is the work (59) on 1-chlorobutadiene-1,2 (XI), which is classified as an ABX_3 case. This compound has been studied by single resonance both at 40 Mc./s. and at 60 Mc./s., and the signs of

(X)

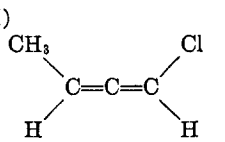

(B) (XI) (A)

J_{AX} and J_{BX} have been shown to be the same (100). The sign of J_{AB} relative to the signs of the other two coupling constants could not be obtained. The additional sign has, however, been obtained by double resonance (59).

The labeling of each transition in the AB and X_3 regions of the spectrum in the limit as all the ratios J_{ij}/δ_{ij} approach zero is given in Table VII. The table shows the spin states of all the other nuclei coupled to the nucleus responsible for a given transition with the assumption that all the coupling constants have the same sign.

TABLE VII

SPIN STATES OF NEIGHBORING NUCLEI FOR ABX_3 SYSTEM FOR COUPLING CONSTANTS ALL THE SAME SIGN

Origin		A							
Transitions		1	2	3	4	5	6	7	8
Spin States	A								
	B	α	α	α	β	α	β	β	β
	X_3	$\alpha\alpha\alpha$	$\alpha\alpha\beta$ $\alpha\beta\alpha$ $\beta\alpha\alpha$	$\alpha\beta\beta$ $\beta\alpha\beta$ $\beta\beta\alpha$	$\alpha\alpha\alpha$	$\beta\beta\beta$	$\alpha\alpha\beta$ $\alpha\beta\alpha$ $\beta\alpha\alpha$	$\alpha\beta\beta$ $\beta\alpha\beta$ $\beta\beta\alpha$	$\beta\beta\beta$

Origin		B							
Transitions		9	10	11	12	13	14	15	16
Spin States	A	α	β	α	β	α	β	α	β
	B								
	X_3	$\alpha\alpha\alpha$	$\alpha\alpha\alpha$	$\alpha\alpha\beta$ $\alpha\beta\alpha$ $\beta\alpha\alpha$	$\alpha\alpha\beta$ $\alpha\beta\alpha$ $\beta\alpha\alpha$	$\alpha\beta\beta$ $\beta\alpha\beta$ $\alpha\beta\beta$	$\alpha\beta\beta$ $\beta\alpha\beta$ $\beta\beta\alpha$	$\beta\beta\beta$	$\beta\beta\beta$

Origin		X_3			
Transitions		17	18	19	20
Spin States	A	α	β	α	β
	B	α	α	β	β
	X_3				

Figures 24a and 25a show the X_3 and AB regions, respectively, of the spectrum of (XI) at 60 Mc./s. with each transition numbered as in Table VII. The A region (lines 1–8) and the B region (lines 9–16) each consists of two overlapping quartets and the X_3 region is a simple quartet (100). Figure 24b shows the change in the X_3 region by selective double irradiation close to lines 4, 6, 7 and 8 of the A region (a sideband frequency of 245 c./s.). This causes collapse of lines 17 and 18. Figure 24c shows the collapse of lines 19 and 20 in the X_3 region by irradiation close to lines 1, 2, 3 and 5 in the A region (a sideband frequency of 258 c./s.). The behavior of the AB region with selective double irradiation of the X_3 region at 245 and 258 c./s. is shown in

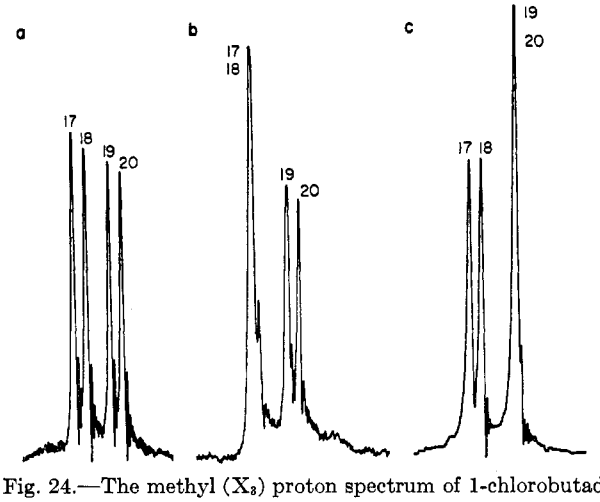

Fig. 24.—The methyl (X_3) proton spectrum of 1-chlorobutadiene at 60 Mc./s.: (a) without double irradiation, (b) with double irradiation at 245 c./s. near lines 4, 6, 7, 8, (c) with double irradiation at 258 c./s. close to lines 1, 2, 3, 5. The lines are numbered as shown in Table VII (59).

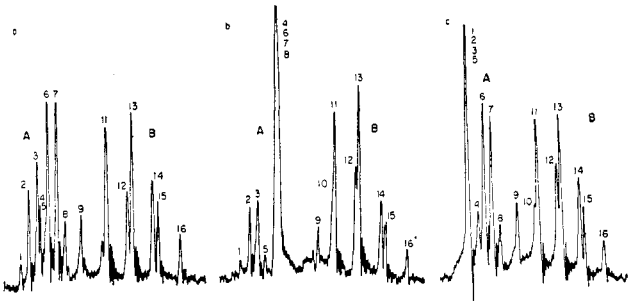

Fig. 25.—The allenic (AB) proton spectrum of 1-chlorobutadiene at 60 Mc./s.: (a) without double irradiation, (b) with double irradiation at 245 c./s., (c) with double irradiation at 258 c./s. (59).

Figures 25b and 25c, respectively. These experiments were carried out with ν_{2x} and $\nu_{2a} = 8.9$ c./s.

To obtain the relative sign of J_{AB} and J_{BX}, Manatt and Elleman (59) assume that irradiation of lines 1, 2, 3 and 5 does not strongly perturb transitions 4, 6, 7 and 8. Then for transitions 1, 2, 3 and 5, nucleus B is in the α state. Thus irradiation of lines 1, 2, 3 and 5 (Figure 24c) should cause collapse of that part of the multiplet in the X_3 region for which nucleus B is in the α state. If J_{AB} and J_{BX} have the same sign, as shown in Table VII, then lines 17 and 18 should collapse. Likewise, when lines 4, 6, 7 and 8 are irradiated while observing the X_3 region (Figure 24b), lines 19 and 20 should collapse. Experimentally what is observed is just the opposite to the behavior predicted from Table VII. Thus J_{AB} and J_{BX} must be opposite in sign. The behavior of the A region when various lines in the X_3 region are irradiated (Figures 25b and 25c) confirms this conclusion.

It was not possible to determine the relative signs of J_{AB} and J_{AX} by decoupling involving the spins B and X. Irradiation of the B region leads to some decoupling of the A and X spins as discussed above for *trans*-crotonaldehyde. In principle it should be possible to obtain the relative signs of J_{AX} and J_{BX} by double irradiation between A and B. However, this was not feasible experimentally because the chemical shift between the A and B regions is only 25 c./s.

Manatt and Elleman (59) made use of Karplus' theoretical work (43, 44) on the contributions of the sigma- and pi-electrons to the coupling constant. They deduced that the absolute signs of J_{AX} and J_{BX} are positive whereas the sign of J_{AB} is negative.

B. $H^1-\{D^2\}$

The magnitudes and relative signs of spin–spin coupling constants in fluorobenzene have been determined by the use of deuterium substitution and $H^1-\{D^2\}$ double resonance, in conjunction with F^{19} resonance studies (10).

The decoupled proton spectrum of 2,3,5,6d_4-fluorobenzene was found to be a single line, not a doublet.

The coupling of the F^{19} atom with the para-hydrogen, J^{HF}_{para}, was therefore 0.0 ± 0.5 c./s.

The normal proton spectrum of 2,4,6d_3-fluorobenzene shows a doublet splitting broadened by deuterium interaction. J^{HF}_{meta}, as obtained from the sharpened doublet of the H^1–$\{D^2\}$ decoupled spectrum, is 5.8 ± 0.2 c./s. The F^{19} resonance spectrum shows the same splitting which arises from coupling with the two equivalent protons. Each component of the 1:2:1 triplet so produced is split further into five lines with the intensity ratios 1:2:3:2:1 by interaction with the two equivalent ortho-deuterium atoms. Since $J^{DF}_{ortho} \sim {}^1/_4 J^{HF}_{meta}$, overlapping of lines occurs and a thirteen-line spectrum is obtained with the intensity ratios 1:2:3:2:3:4:6:4:3:2:3:2:1. J^{DF}_{ortho} is found to be about 1.4 ± 0.1 c./s., so that J^{HF}_{ortho} must be 9.0 ± 0.7 c./s.

The measurements of the coupling constants were improved slightly by the complete analysis of the spectra of fluorobenzene and 4d-fluorobenzene and by H′-$\{F^{19}\}$ double resonance. In addition, the signs of the above coupling constants and of the proton–proton coupling constants were found to be the same from the second-order spectrum obtained at 30 Mc./s.

c. H^1–$\{B^{11}\}$

The double resonance method has been of great value in the assignment of the n.m.r. spectra of the boron hydrides and the borohydride ion. These spectra are complicated by the large numbers of magnetic nuclei and non-equivalent positions involved. In all cases large amplitudes of H_2 have been used and the chemical shifts have not been measured accurately by the double resonance technique.

The equivalence of the four protons in the sodium borohydride molecule (62) was confirmed by decoupling the B^{11} and proton spins (93). The normal proton spectrum consists of a quartet with components of equal intensity due to spin-coupling with one B^{11} nucleus ($I = 3/2$), and of a less intense septet due to splitting by B^{10} (natural abundance 18%, $I = 3$). The quartet is collapsed to one line by H^1–$\{B^{11}\}$ spin decoupling. The B^{10} structure of course remains.

The normal proton spectrum of diborane is asymmetrical and cannot arise from an ethane-like model. The H^1–$\{B^{11}\}$ decoupled spectrum consists of two lines. There are thus two types of protons present in the molecule, and from the spectral intensities their relative numbers are deduced to be in the ratio of 2:1. These observations fit the bridge model which has been established by electron diffraction (39) and infrared (75) investigations. The proton shifts are most accurately derived from the double resonance spectrum, and the coupling constants only from the B^{11} spectrum. All the features of the normal proton spectrum then can be assigned.

In pentaborane-9, B_5H_9, there are two types of borons in the ratio of 4:1, as shown by the B^{11} spectrum, and three types of protons as shown by the decoupled proton spectrum (86, 93). Two of the three kinds of protons give equally intense signals in the appropriate decoupled spectrum. The third gives a less intense signal. Because of the different shifts of the B^{11} nuclei in the two locations, only one type of B^{11} nucleus at a time could be decoupled completely from the protons in a field-sweep experiment, so that the relative intensities of the proton signals are not immediately obvious. However, there are only two possibilities: 4:4:1 and 3:3:2. The former fits the structure determined by X-ray analysis (53). This structure has a square-pyramidal framework of borons, the apical boron being bonded to only one proton, and each of the four basal borons being bonded to one terminal and two bridge protons.

The normal proton spectra of B_5H_8Br and B_5H_8I do not contain the features which in the B_5H_9 spectra are associated with the apical proton. It is concluded that the apical proton has been replaced. This is confirmed both by the H–$\{B^{11}\}$ spectra and the B^{11} spectra. Decoupling occurs at only *one* frequency corresponding to the resonance frequency of the *basal* boron atoms. In the B^{11} spectrum of B_5H_9, two doublets of relative intensity 4:1 are obtained corresponding to the four basal borons and one apical boron, respectively. Whereas in B_5H_9 the apical boron signal is a doublet due to splitting by the apical proton, in B_5H_8Br and B_5H_8I the same signal is not split since the apical proton has been replaced (87).

The more structurally complex molecules pentaborane-11, B_5H_{11}, and decaborane, $B_{10}H_{14}$, also have been studied with the aid of H^1–$\{B^{11}\}$ decoupling techniques. Despite the known structure of these compounds (53), opinions as to the interpretation of the H^1 and B^{11} spectra differ, and the spectra cannot be fully assigned (52, 86, 107). It was, however, possible to decide that in the halides $B_{10}H_{13}Br$ and $B_{10}H_{13}I$, the halogen atoms are attached to the B2 borons (87) (in the notation of Kasper, Lucht and Harker (45)).

An interesting example of the successful use of a number of different n.m.r. experiments, including H^1–$\{B^{11}\}$ double resonance, is the work of Shoolery on the molecule $(CH_3)_2PH{\cdot}BH_3$ (93). This molecule contains fourteen nuclei, twelve of which have magnetic moments and eleven of which are spin coupled to the P^{31} nucleus ($I = 1/2$). The structure and six of the ten coupling constants were obtained from four spectra: the normal proton spectrum, the H–$\{B^{11}\}$ decoupled spectrum, the B^{11} spectrum, and the P^{31} spectrum.

The P^{31} spectrum shows two groups of resonances, each unresolved, with a separation of 350 cycles. The H^1–$\{B^{11}\}$ decoupled spectrum contains this same split-

ting which may thus be assigned to a P–H coupling. The large value of the interaction indicates that these nuclei are linked directly. The doublet is also present of course in the normal proton spectrum. Four other features of the normal proton spectrum are absent from the decoupled spectrum and may be assigned to protons (H_b) attached to boron. The number of these protons can be deduced to be three from the B^{11} spectrum, which consists of two overlapping quartets. Each quartet has the intensity ratios 1:3:3:1 and is ascribed to splitting by three equivalent protons. The added doublet splitting is due to the P^{31} nucleus.

In the decoupled spectrum the phosphine-proton has multiplet structure. This is due to splitting by six equivalent protons in two methyl groups. The methyl groups are responsible for the most intense signal in the proton spectrum. This signal consists of two doublets, one splitting being due to the phosphine-proton and one to the P^{31} nucleus. These facts fit the structure

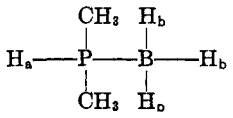

The derived coupling constants are given in Table VIII.

TABLE VIII
COUPLING CONSTANTS DETERMINED FOR $(CH_3)_2PH \cdot BH_3$

Spectrum	J_{HP}	J_{HH_a}	J_{PH_a}	J_{BH_b}	J_{BP}	J_{PH_b}
H^1	12	6		90		12
H^1–{B^{11}}	12	6	350			
B^{11}				90	50	
P^{31}			350			

It was observed that the H_a signals become more intense when the B^{11} nucleus is irradiated, and, moreover, then are resolved into a multiplet. This indicates that there is an additional coupling, J_{BH_a}, which is not resolved in the normal proton spectrum nor in the B^{11} spectrum.

An additional example of H^1–{B^{11}} decoupling is considered in section V-H.

D. H^1–{C^{13}}

The value of the ratio of the magnetogyric ratios of C^{13} and H^1 obtained by Poss (72) was confirmed and the accuracy improved by a double irradiation experiment (84). A sample of methyl iodide enriched to 51% with C^{13} was used. The value 0.251443 ± 0.0000005 for the ratio $\gamma_{C^{13}}/\gamma_{H^1}$ was found, in agreement with the previous figure of 0.25143 ± 0.000005. The doublet nature of the normal proton spectrum confirmed the value 1/2 for the nuclear spin of the C^{13} nucleus. This value had been obtained by Jenkins from hyperfine-structure measurements (41).

E. H^1–{N^{14}}

1. *Amides*

(a) Formamide

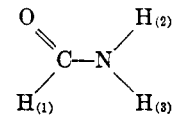

The double resonance technique was applied by Piette, Ray, and Ogg to determine the proton spin–spin coupling constants in formamide (65). The normal proton resonance spectrum of formamide at 40 Mc./s. as shown in Figure 26a is considerably broadened because of coupling of the protons to the N^{14} nucleus. The effect of H^1–{N^{14}} double resonance on the proton spectrum is shown in Figure 26b.

The double irradiation experiment shows that the amine protons in formamide, like the methyl groups in N,N-dimethylformamide, are inequivalent because of restricted rotation about the C—N bond. Taking $H_{(1)}$ as the formyl hydrogen, the coupling constants J_{12} and J_{13} were found to be 13 c./s. and 2.1 c./s. in the pure liquid. The larger coupling constant was attributed to the *trans* coupling. This assumption has been proven to be correct by an H^1–{N^{14}} study of N-methylformamide (see Section V-E-1b) (80).

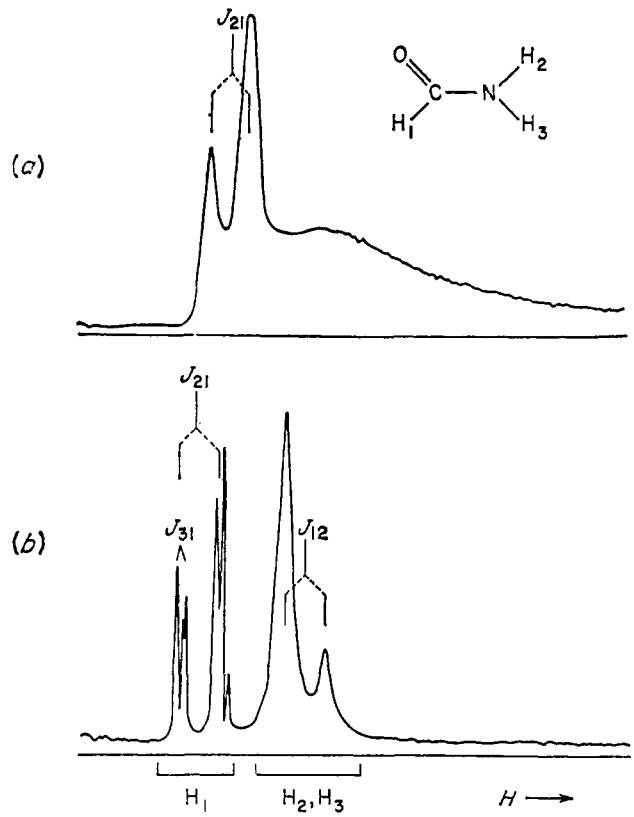

Fig. 26.—The proton spectrum of formamide at 40 Mc./s. with (a) N^{14} not decoupled and (b) double irradiation at the N^{14} resonance frequency, 2.8904 Mc./s. (65).

The signal due to $H_{(3)}$ in the H–$\{N^{14}\}$ decoupled spectrum of formamide overlaps one component of the $H_{(2)}$ doublet at 40 Mc./s. The other component is broad and the splitting J_{23} could not be resolved. This splitting, however, has been resolved in the case of N^{15}-substituted formamide (99). Its value is 2.4 c./s. The broadening of the amine resonance in the N^{14} case is thus not due to exchange effects since these would be operative also in the N^{15} molecule. The broadening presumably is the result of incomplete decoupling of the N^{14} nucleus.

The line-width of the formyl proton is also of interest. At 60 Mc./s. the small splitting J_{13} cannot be resolved. The broadening must here be attributed, as for the amine proton, to coupling with the N^{14} nucleus, since double irradiation sharpens the formyl signals (82). The effect may also be observed in the published spectra at 40 Mc./s. of Piette, Ray and Ogg (65) as shown in Figure 26, but, because the NH and CH proton resonances overlap at 40 Mc./s. in the undecoupled case, this result is not as obvious.

The $H_{(3)}$ signal moves to low-field in water solution and no longer overlaps the $H_{(2)}$ doublet. Once more the splitting J_{23} was not resolved even in the decoupled spectrum. Deuterium substitution of the formyl hydrogen also enabled the $H_{(2)}$ and $H_{(3)}$ resonances to be separated. There was a suggestion of a triplet structure due to $J_{(D_1-H_2)}$ on the $H_{(2)}$ signal (65).

Partial deuteration at the amine positions gave a mixture of products, and the spectrum of the mixture was a superposition of the spectra of D_2NCHO, DHNCHO, and H_2NCHO (65).

(b) N-Methylformamide

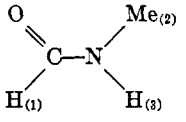

The proton–proton coupling constants in N-methylformamide have been determined similarly with the aid of H^1–$\{N^{14}\}$ decoupling (80). The normal proton spectrum at 60 Mc./s. of N-methylformamide consists of a high-field quartet and two broad low-field features which overlap in the case of the pure liquid. The high-field quartet is assigned to the methyl-group protons. The broader of the low-field features is assigned to the NH proton.

The effect of H^1–$\{N^{14}\}$ decoupling on the low-field features of the spectrum is shown in Figure 27. Not only is structure seen on the sharpened NH signal but the low-field signal of the formyl proton is similarly sharpened and is shown to contain structure. It follows that both the amine and the formyl protons are spin-coupled to the nitrogen. The methyl proton signals, however, are unaffected by the decoupling and are thus not appreciably coupled to the nitrogen.

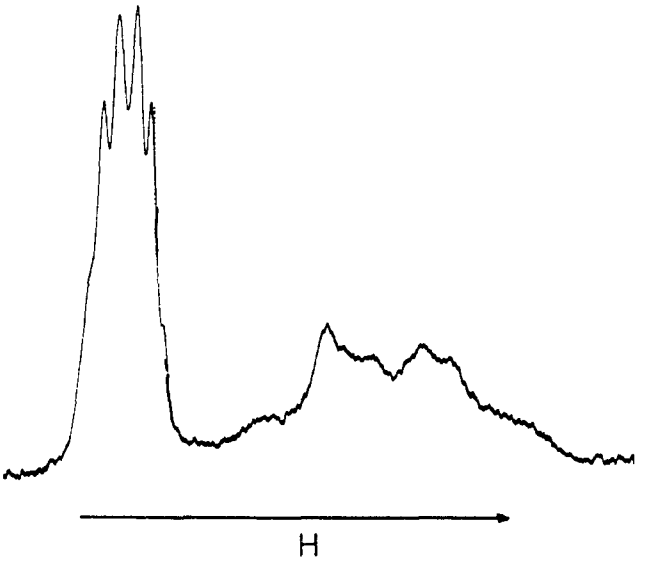

Fig. 27.—CH and NH proton resonances of N^{14} decoupled N-methylformamide (pure) at 60 Mc./s. (80).

The H^1–$\{N^{14}\}$ decoupled spectrum can be analyzed as an ABX_3 system. The derived coupling constants for the pure liquid are: $J_{13} = 1.8$ c./s.; $J_{23} = 4.9$ c./s.; $J_{12} = 0.9$ c./s.

If the stable configuration of N-methylformamide has the methyl group *trans* to the formyl hydrogen (55) then the double resonance work confirms the assignments of the spectra of formamide (65, 99) and N,N-dimethylformamide (46). The coupling constants between the CH and the two NH protons in pure N^{15} formamide are 2.1 c./s. and 12.9 c./s. (99). By analogy with N-methylformamide the low value of 2.1 c./s. must be assigned to J_{13} in formamide. Thus $J_{trans} > J_{cis}$ in formamide, as in the ethylenic compounds (43), as was assumed (65, 99). The coupling constant $J_{12} = 0.9$ c./s. for N-methylformamide can, of course, be compared with the values 0.4 c./s. and 0.8 c./s. for the coupling of the CH proton to the two methyl groups in N,N-dimethylformamide (46) to suggest the assignment of the 0.8 c./s. coupling to J_{12}. Again $J_{trans} > J_{cis}$ for the long-range coupling constant.

The relative signs of J_{12} and J_{23} were found by comparison of the spectrum of the methyl group at 40 Mc./s. with spectra for like and opposite signs of these coupling constants. The calculated and observed spectra are shown in Figure 28 (80). The sign of J_{12} is opposite to that of J_{23}.

Dilution of N-methylformamide in water produces large changes in the proton chemical shifts. Though chemical shifts are always dependent on the details of solvent interactions, coupling constants are usually not solvent dependent. However, J_{13} for N-methylformamide changes from 1.8 ± 0.1 c./s. in the pure liquid to 2.3 ± 0.1 c./s. for a 33 volume per cent solution in water. The variation has a marked effect upon the appearance of the CH group resonance since it deter-

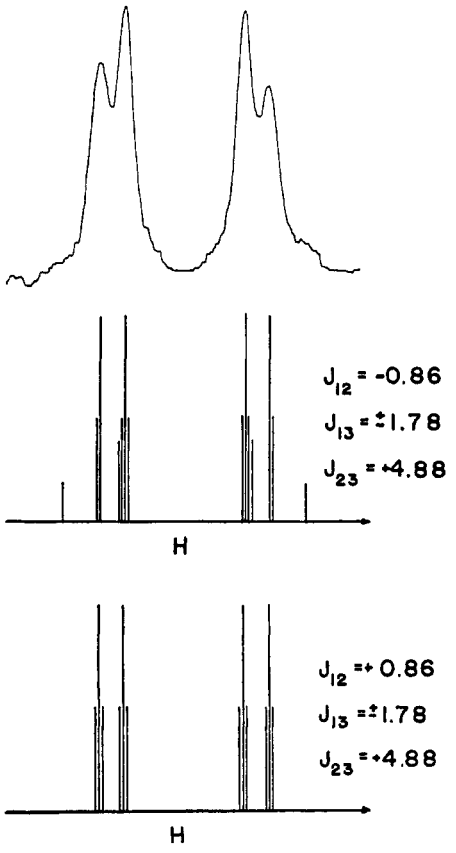

Fig. 28.—CH_3 proton resonance of N-methylformamide (pure) at 40 Mc./s., with spectra calculated for like and opposite signs of J_{12} and J_{23}. The calculated spectra are invariant with change in sign of J_{13} (80).

mines the extent to which the two quartets of the signal overlap. This may be seen from a comparison of Figures 27 and 29. For the pure liquid only six peaks can be observed whereas for the water solution seven peaks are discernible. It can be argued from these results and the theory of Karplus (43) that dilution of N-methylformamide in water favors the resonance form

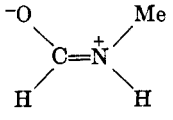

The results of Randall and Baldeschwieler (80) are consistent with the work of Fraenkel and Franconi, who have found that protonation of amides in acid solution occurs at the oxygen and leads to an increase in J_{13} (28).

(c) N,N-Dimethylformamide

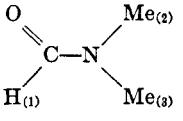

A double resonance effect on the CH resonance in

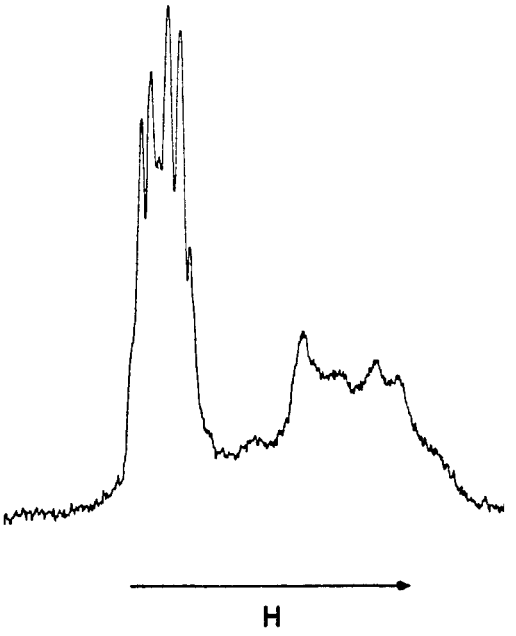

Fig. 29.—CH and NH proton resonances of N^{14} decoupled N-methylformamide (33% by volume in water) at 60 Mc./s. (80).

N,N-dimethylformamide (80) has been found as for the formamide (82) and N-methylformamide cases (80). The normal and decoupled proton spectra of the formyl group at 60 Mc./s. are shown in Figure 30. Double irradiation decreases the half-width from 2.9 to 2.4 c./s. Unfortunately, the structure of the CH resonances cannot be completely resolved.

(d) Acetamides

Double resonance effects at the amine protons of both acetamide and N-methylacetamide have been observed (80). Unfortunately, even with $H^1-\{N^{14}\}$ decoupling, the structure of the NH signals could not be resolved completely.

(e) N^{14} Chemical Shifts

The N^{14} resonance frequencies for all the amides con-

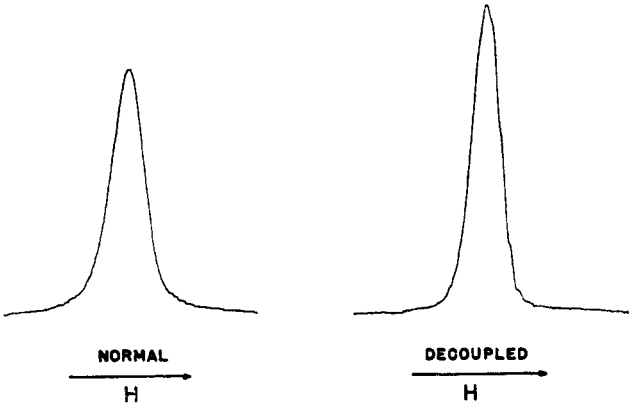

Fig. 30.—Normal and N^{14} decoupled CH proton resonance of N,N-dimethylformamide (pure) at 60 Mc./s. (80).

sidered above were found to be the same to within the rather large error, ± 10 c./s., of the measurement (80).

2. *Pyridine and Pyridinium Ion*

The H^1–$\{N^{14}\}$ double resonance effect in pyridine has been found by observation of the α-proton resonances, which are quadrupolar broadened by the N^{14} nucleus, as shown in Figure 31 (81). The decoupled

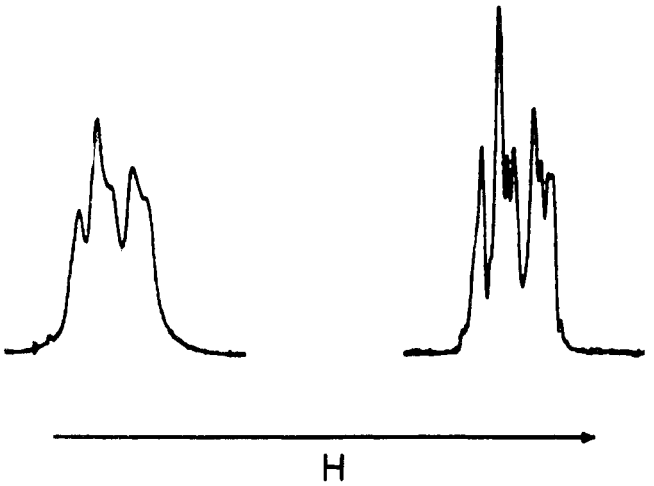

Fig. 31.—α-Proton resonance of pyridine (pure liquid) at 40 Mc./s. without and with double resonance (81).

spectrum for pyridine agrees very well with the previously calculated spectrum (90, 91).

In the case of the pyridinium ion the double resonance effect of the amine–proton signal was observed as shown in Figure 32 (81). The normal proton spectrum

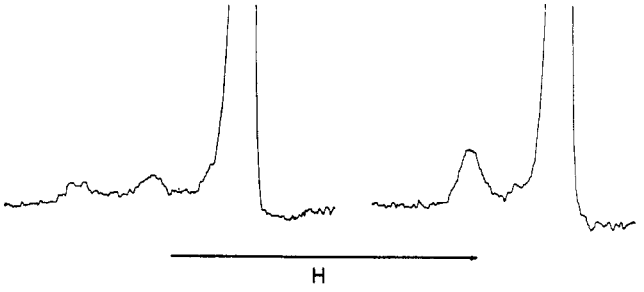

Fig. 32.—Amine–proton resonance of pyridinium ion in trifluoroacetic acid at 40 Mc./s. without and with double resonance (81).

of the amine proton is a broadened triplet for a 5% solution of pyridine in trifluoroacetic acid. At higher concentrations of pyridine, the triplet is not obtained because of faster proton exchange (96). The CH proton resonances of the ion are all broad. Double irradiation had no effect upon the 40 Mc./s. spectrum of these protons, however. The main broadening is therefore not quadrupolar but may be attributed to exchange effects of the amine proton. An exchange rate of several $sec.^{-1}$ would be fast enough to broaden the ring proton resonances which have coupling constants of the order of several c./s., and yet would enable the amine proton triplet with a splitting of 70 c./s. to be observed.

The N^{14} chemical shifts in these molecules were determined and compared with the shifts in NH_3 and NH_4^+ (81). Table IX shows the results. The low-

TABLE IX

N^{14} CHEMICAL SHIFT MEASUREMENTS OBTAINED BY H–$\{N^{14}\}$ DOUBLE RESONANCE

Molecule	NH_3	NH_4^+	$C_5H_6N^+$	C_5H_5N
Shift, p.p.m.	16.8 ± 0.5	0.0	−175.6 ± 1	−293.3 ± 10

field value of the shift for pyridine relative to the pyridinium ion probably is due to a larger paramagnetic contribution to the pyridine shift arising because the energy required to promote an electron to the first excited state presumably is much less in pyridine than in any of the other molecules considered. The paramagnetic term may also affect the α-proton chemical shifts (81).

3. *Pyrrole*

The N–H proton resonance in pyrrole normally is difficult to detect because it is broadened by a quadrupole relaxation mechanism. The H^1–$\{N^{14}\}$ double resonance effect in this molecule has been observed by Shoolery (94). The N–H proton in the decoupled spectrum of the pure liquid was partially resolved into a broadened multiplet. In addition, the resolution of the signals of both the α- and β-protons was improved by the decoupling. This indicates that both types of ring-protons are appreciably coupled to the nitrogen nucleus. A few other cases of broadening of resonances of protons not directly bonded to the quadrupolar nucleus have been considered in other sections. These cases were: the formyl-protons in formamide, N-methylformamide, and N,N-dimethylformamide; and the phosphine proton in $(CH_3)_2PH \cdot BH_3$.

The enhancement of the intensity of the NH proton signal by decoupling has been used by Happe in the measurement of the solvent effect on the N–H proton shifts (38). Upon dilution of pyrrole with cyclohexane, all the proton resonances move to low field. The NH signal moves most and the β-ring proton signal least. This is consistent with the breakup of "π-interactions" between the N–H proton of one pyrrole molecule and the π-electrons of a second molecule. Happe has analyzed the data further and deduces that the association is dimeric in dilute solution and that in each dimer each NH is bonded to the π-electrons of the other ring.

Happe also observed that the addition of pyridine resulted in a shift of the NH proton signal to lower fields. This was taken to indicate that the pyrrole–pyridine association is of the "n-donor" type and in-

volves the lone-pair electrons of the nitrogen in the pyridine ring. An equilibrium constant of 23.1 at 33° for the association was determined from a study of the temperature dependence of the shift. This agrees with the value of 22 ± 3 at 30° obtained from infrared measurements on CCl_4 solutions (103).

4. Ammonia and the Ammonium Ion

The first double resonance spectra for the ammonium ion were obtained by Anderson, Pipkin and Baird (7). The theoretical treatment of the $H-\{N^{14}\}$ double resonance spectra of $N^{14}H_3$ has been given by Baldeschwieler (12) and has been considered already in Section II-A-3.

The treatment was extended to the case of $N^{14}H_4^+$ and the theoretical spectra at intermediate values of H_2 and at various values of ω_2 were determined (14). Good agreement between experiment and theory was obtained as shown for example by Figure 5 in section III-B-2. The N^{14} chemical shifts in NH_3 and NH_4^+ were also found and have been discussed in section V-E-2.

F. $H^1-\{N^{15}\}$

Anderson, Pipkin and Baird obtained $H^1-\{N\}$ double resonance spectra for both $N^{14}H_4^+$ and $N^{15}H_4^+$ and, by measurement of the frequency of the decoupling fields for the two molecules, were able to determine the relative value of the magnetogyric ratios of the N^{14} and N^{15} nuclei (7). The value obtained was

$$\gamma_{N^{15}}/\gamma_{N^{14}} = 1.4027576 \pm 15 \times 10^{-7}$$

The accuracy was improved by Baldeschwieler (14) who obtained the value

$$\gamma_{N^{15}}/\gamma_{N^{14}} = 1.40275480 \pm 20 \times 10^{-8}$$

The behavior of the $N^{15}H_4^+$ system at various values of H_2 and ω_2 was determined both experimentally and theoretically (14). Figure 6 (section III-B-2) shows the good agreement between the two.

G. $H^1-\{F^{19}\}$

Lauterbur has used a second field of large amplitude at the F^{19} resonance frequency to simplify the proton spectrum of the molecule $(CF_3CH_2CH_2SiMeO)_3$. The spectrum of the $-CH_2CH_2-$ group was reduced to a simple A_2B_2 case by irradiation of the fluorine nuclei.

The normal proton spectrum of *sym*-trifluorobenzene is complicated by the long-range H–F couplings (95). The $H^1-\{F^{19}\}$ decoupled spectrum has only one line since all the hydrogens are equivalent to each other. Only one decoupling frequency is needed since all the fluorines also are equivalent.

H. $H^1-\{Al^{27}\}$

The n.m.r. study of a number of compounds containing aluminum, boron, and hydrogen is interesting because two different decoupling experiments were used (63). These were $H^1-\{B^{11}\}$ and $H^1-\{Al^{27}\}$ decoupling.

The first compound studied, which we shall call A, was prepared by the method of Schlesinger, Sanderson, and Burg (89). It has been analyzed as AlB_3H_{12} and has been called aluminum borohydride. The most probable structure (76, 17) for this compound *in the vapor* is one of D_3 (or D_{3h}) symmetry, and presumably consists of three distorted tetrahedral BH_4 units each bonded to aluminum by two hydrogen bridges. The boron atoms form an equilateral triangle with the aluminum atom at the center.

The normal proton spectrum for A in the liquid phase is a single broad peak that is not temperature dependent. It is narrowed slightly by $H^1-\{B^{11}\}$ decoupling. The decoupled spectrum contains unresolved structure presumably arising from H^1-Al^{27} spin–spin coupling. If this is so, J_{Al-H} must be of the order of 40 c./s. The $H^1-\{Al^{27}\}$ spectrum resembles the normal proton spectrum of the borohydride ion. It was deduced that the protons are all equivalent and are all bonded to B^{11} (63). The B^{11} spectrum resembles the corresponding B^{11} spectrum of the BH_4^- ion, *i.e.*, it is a quintuplet.

The experimental data are difficult to fit to the structure as derived by gas-phase methods since equivalence of the proton resonances would require a dynamical process to average out the chemical shifts for the inequivalent positions. Such a process should be temperature dependent whereas the proton spectrum is not. Ray and Ogg invoke a "quantum-mechanical tunneling process." However, it may be queried whether A in the liquid has the same structure as deduced by the gas-phase methods. It is also possible that the protons are in fact not equivalent (5).

Similar considerations apply to a second compound, B, which Ogg and Ray (63) obtained from A by first heating and then rapid cooling. The work is currently under reinvestigation (61).

I. $H^1-\{P^{31}\}$

The coupling constants of the methylene groups with the methyl protons and with the P^{31} nucleus in triethyl phosphite have been shown to be nearly equal by spin decoupling (95). The normal n.m.r. spectrum of the methylene groups is a rather symmetrical five line pattern. With $H^1-\{P^{31}\}$ double resonance, the spectrum of the methylene groups is reduced to a four-line multiplet arising from coupling with the methyl groups. From this result it is clear that the five-line pattern arises from the overlap of two quartets, and that $J_{CH_2-P^{31}}$ and $J_{CH_2-CH_2}$ must be equal.

J. $H^1-\{Pb^{207}\}$

The proton spectrum at 30 Mc./s. of lead tetraethyl has been studied by Baker (11). An $H^1-\{Pb^{207}\}$ de-

coupling experiment was used to determine the ratio $\gamma_{Pb^{207}}/\gamma_{H_1}$. The value obtained was 0.2092198 ± 10×10^{-7}.

K. B^{11}–$\{B^{10}\}$

Only one example of B^{10}–B^{11} spin–spin coupling has been reported (106). This was for tetraborane, B_4H_{10}. This molecule appeared to be the most favorable case for which B^{10}–B^{11} coupling could be detected since it is the only boron hydride which has only one type of single-bond between borons.

The B^{11} spectrum includes a low-field triplet arising from B–H coupling in the two terminal BH_2 groups, and a high-field doublet arising from B–H coupling in the two central BH groups. Each feature of the BH_2 triplet shows a barely resolved triplet arising from the two equivalent bridging protons. Each component of the BH doublet similarly contains unresolved fine structure.

B^{11}–$\{B^{10}\}$ double resonance has been used (83) to test the assignment of this fine structure to B^{10}–B^{11} spin–spin coupling. Irradiation of the sample at about the B^{10} resonance frequency did not remove the fine structure and the above assignment is not confirmed. Deuteration of the molecule, on the other hand, did remove this structure which may thus be attributed to a spin-spin interaction with H^1.

L. C^{13}–$\{H^1\}$

The collapse of spin-multiplets in the C^{13} spectra of a number of organic molecules by C^{13}–$\{H^1\}$ double resonance has been accomplished by Lauterbur (50). Figure 33 shows the effect for methyl iodide, cyclohexane and benzene.

Positive Overhauser effects were found for these and other molecules, and the enhancement factors are given in Table X.

TABLE X

NUCLEAR OVERHAUSER ENHANCEMENT FACTORS FOR C^{13}–$\{H^1\}$ EXPERIMENTS[a]

Molecule	Enhancement factor[b]
CH_3I (60% C^{13} enrichment)	0.7
HCOOH (88% solution in H_2O)	2.0
C_6H_6	2.0
1,3,5-Trimethylbenzene (2,4,6-C^{13} resonances)	1.0
$Sn(CH_3)_4$ (methyl C^{13}-resonances)	0.8

[a] Measurements were made under rapid passage dispersion mode conditions with C^{13} in natural abundance except as noted for CH_3I, H_2 = 320 milligauss.

[b] The enhancement factor is defined as: $(a - a_0)/a_0$ where a_0 is C^{13} signal intensity before double resonance; a is C^{13} signal intensity with C^{13}–$\{H^1\}$ double resonance.

M. C^{13}–$\{F^{19}\}$

The only known example of a C^{13}–$\{F^{19}\}$ double resonance experiment is the work of Lauterbur on trifluoroacetic acid (50). This case already has been considered in Section III-B-2.

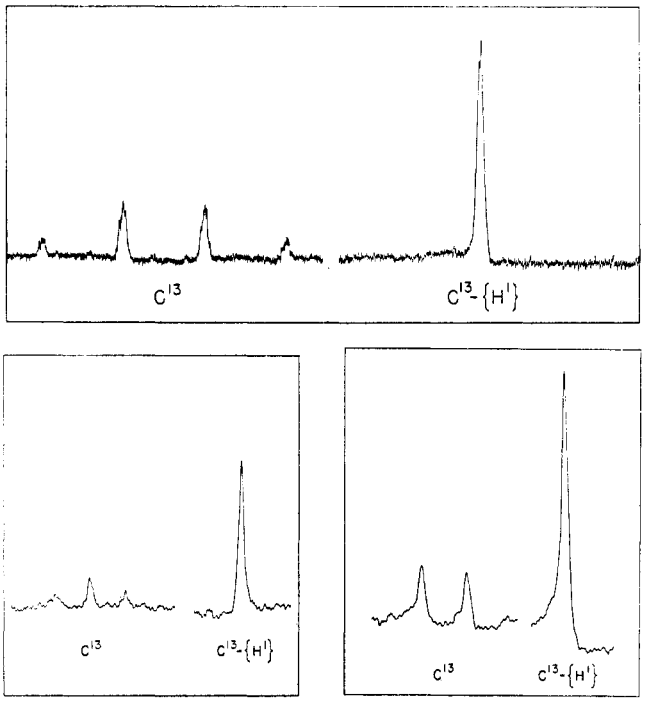

Fig. 33.—C^{13} spectra of (a) methyl iodide, (b) cyclohexane, and (c) benzene, without and with double irradiation at the proton resonance frequency (50).

N. F^{19}–$\{N^{14}\}$

The decoupled F^{19} spectra for the molecules NF_3, N_2F_4 (16) and the two forms of N_2F_2 (15) have been obtained. In the limit of large H_2, a single peak results in all cases. For N_2F_4 this result together with the microwave results (51) indicate that the barrier to rotation of the NF_2 groups with respect to each other is very low.

Of the two forms of N_2F_2 the stable form has been shown to have a *trans* structure (27, 85). Two structures have been proposed for the unstable isomer: a *cis* form; and a 1,1-difluoro structure (27, 85). The undecoupled F^{19} spectrum of the unstable isomer in CCl_3F solution at 40 Mc./s. is shown in Figure 34a. The spectrum consists of five lines, indicating that both nitrogens must be coupled to the fluorines if the molecule is of the 1,1-difluoro form, or that the molecule represents a complicated example of an AXX′A′ case where the fluorine and nitrogens are not magnetically equivalent (69), if the molecule has the *cis* structure. As has been noted in section III-B-2, if the nitrogen nuclei have the same resonance frequency ν_{oN}, then double resonance spectra recorded by sweeping field will be mirror images when $\omega_2/2\pi$ is set at equal frequency intervals above and below $\omega_2/2\pi = \nu_{oN}$. This readily observed regularity of the double resonance spectrum will not occur if $\nu_{oN} \neq \nu_{oN'}$.

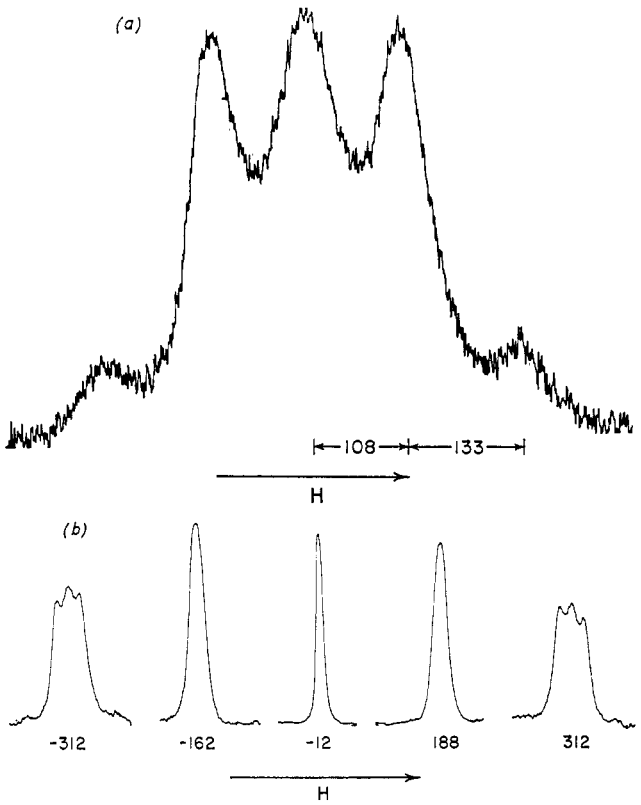

Fig. 34.—(a) F^{19} spectrum of *cis*-N_2F_2 at 40 Mc./s. without double resonance; (b) F^{19}-$\{N^{14}\}$ double resonance spectra of *cis* N_2F_2 at several values of A_N in c./s. (15).

The double resonance spectra of the unstable isomer at several values of $\omega_2/2\pi$ above and below ν_{oN} are shown in Figure 34b. These results indicate that $\nu_{oN} = \nu_{oN'}$. Thus the 1,1-difluoro structure is quite improbable.

O. F^{19}–$\{P^{31}\}$

Bloom and Schoolery investigated the F^{19}–$\{P^{31}\}$ double resonance spectra of Na_2PO_3F both at various values of ω_2 as well as H_2 (22). Good agreement between the calculated and observed spectra was obtained.

P. Sn^{119}–$\{H^1\}$

One example of decoupling involving Sn^{119} is known. It is for the molecule tetramethyltin (50). The spectra obtained under rapid passage dispersion mode conditions are shown in Figure 35.

The authors wish to thank Miss Bethia C. Reynolds for her assistance in the preparation of this manuscript. The financial support of the National Science Foundation, and the Office of Naval Research for one of us (E.W.R.), are gratefully acknowledged.

The authors thanks also are given to Drs. P. C. Lauterbur, S. L. Manatt, D. D. Elleman, R. Freeman, D. H. Whiffen, D. W. Turner, and J. N. Shoolery for sending us preprints of their publications, unpublished spectra, and figures used in this review.

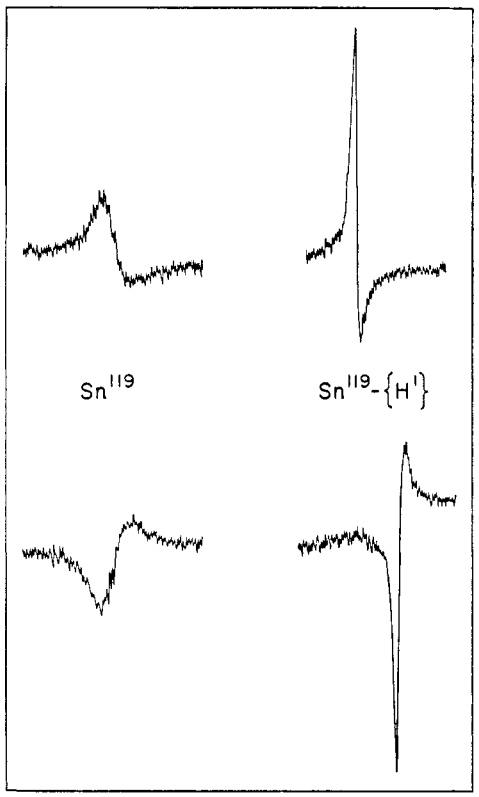

Fig. 35.—Sn^{119} spectra of tetramethyltin without and with double irradiation at the proton resonance frequency (50).

Finally the authors wish to thank the American Chemical Society for permission to reproduce Figures 10, 11, 12, 13, 24, and 25; The American Institute of Physics for Figures 2, 5, 6, 7, 9, 17, 18, 19, and 20; The Chemical Society for Figures 31 and 32; The Physical Society for Figure 1; Academic Press, Inc., for Figures 26, 27, 28, 29, and 30; and Taylor and Francis, Ltd., for Figures 14, 15, 16, 21, 22, and 23.

VI. REFERENCES

(1) Abragam, A., *Phys. Rev.*, **98**, 1729 (1955).
(2) Abragam, A., "The Principles of Nuclear Magnetism," Oxford University Press, New York, N. Y., 1961, p. 530.
(3) Abragam, A., Ref. 2, p. 533.
(4) Abragam, A., Ref. 2, p. 535.
(5) Abraham, R. J., and Bernstein, H. J., *Can. J. Chem.*, **39**, 216 (1961).
(6) Abraham, R. J., Freeman, R., McLauchlan, K. A., and Hall, L. D., *J. Chem. Soc.*, 2080 (1962).
(7) Anderson, L. W., Pipkin, F. M., and Baird, J. C., *Phys. Rev.*, **116**, 87 (1953).
(8) Anderson, W. A., *Phys. Rev.*, **102**, 151 (1956).
(9) Anderson, W. A., and Johnson, L. F., "Special Operating Techniques," Varian Associates, Palo Alto, Calif., 1959.
(10) Bak, B., Shoolery, J. N., and Williams, G. A., *J. Mol. Spectroscopy*, **2**, 525 (1958).
(11) Baker, E. B., *J. Chem. Phys.*, **26**, 960 (1957).
(12) Baldeschwieler, J. D., *J. Chem. Phys.*, **34**, 718 (1961).
(13) Baldeschwieler, J. D., and Fulton, R. L., *J. Chem. Phys.*, **34**, 1075 (1961).
(14) Baldeschwieler, J. D., *J. Chem. Phys.*, **36**, 152 (1962).

(15) Baldeschwieler, J. D., Noggle, J. H., and Colburn, C. B., *J. Chem. Phys.*, **37**, 182 (1962).
(16) Baldeschwieler, J. D., Randall, E. W., and Colburn, C. B., unpublished work.
(17) Bauer, S. H., *J. Am. Chem. Soc.*, **72**, 622 (1950).
(18) Bloch, F., *Phys. Rev.*, **70**, 460 (1946).
(19) Bloch, F., *Phys. Rev.*, **94**, 496 (1954).
(20) Bloch, F., *Phys. Rev.*, **102**, 104 (1956).
(21) Bloch, F., and Siegert, A., *Phys. Rev.*, **57**, 522 (1940).
(22) Bloom, A. L., and Shoolery, J. N., *Phys. Rev.*, **97**, 1261 (1955).
(23) Corio, P. L., *Chem. Rev.*, **60**, 363 (1960).
(24) Cotton, J. F., and Klapper, H., private communication.
(25) Elleman, D. D., and Manatt, S. L., *J. Chem. Phys.*, **36**, 2346 (1962).
(26) Elvidge, J. A., and Jackman, L. M., *J. Chem. Soc.*, 859 (1961).
(27) Ettinger, R., Johnson, F. A., and Colburn, C. B., *J. Chem. Phys.*, **34**, 2187 (1961).
(28) Fraenkel, G., and Franconi, C., *J. Am. Chem. Soc.*, **82**, 4478 (1960).
(29) Freeman, R., *Mol. Phys.*, **3**, 435 (1960).
(30) Freeman, R., *Mol. Phys.*, **4**, 385 (1961).
(31) Freeman, R., and Pound, R. V., *Rev. Sci. Instr.*, **31**, 103 (1960).
(32) Freeman, R., and Whiffen, D. H., *Mol. Phys.*, **4**, 321 (1961).
(33) Freeman, R., and Whiffen, D. H., *Proc. Phys. Soc.*, **79**, 794 (1962).
(34) Glassel, J. A., Turner, D. W., and Jackman, L. M., *Proc. Chem. Soc.*, 426 (1961).
(35) Guthrie, R. D., unpublished results.
(36) Gutowsky, H. S., McCall, D. W., and Slichter, C. P., *J. Chem. Phys.*, **21**, 279 (1953).
(37) Hahn, E. L., and Maxwell, D. E., *Phys. Rev.*, **88**, 1070 (1952).
(38) Happe, J. A., *J. Phys. Chem.*, **65**, 72 (1961).
(39) Hedberg, K., and Schomaker, V., *J. Am. Chem. Soc.*, **73**, 1482 (1951).
(40) Itoh, J., and Sato, S., *J. Phys. Soc. Japan*, **14**, 851 (1959).
(41) Jenkins, F. A., *Phys. Rev.*, **72**, 169 (1947).
(42) Kaiser, R., *Rev. Sci. Instr.*, **31**, 963 (1960).
(43) Karplus, M., *J. Chem. Phys.*, **30**, 11 (1959).
(44) Karplus, M., *J. Chem. Phys.*, **33**, 1842 (1960).
(45) Kaspar, J. S., Lucht, C. M., and Harker, D., *Acta Cryst.*, **3**, 436 (1950).
(46) Kowalewski, V. J., and de Kowalewski, D. G., *J. Chem. Phys.*, **32**, 1272 (1960).
(47) Kowalewski, V. J., and de Kowalewski, D. G., *J. Chem. Phys.*, **33**, 1794 (1960).
(48) Lauterbur, P. C., "Determination of Organic Structures by Physical Methods," Academic Press, Inc., New York, N. Y., 1962, Chap. 7, p. 531.
(49) Lauterbur, P. C., *J. Chem. Phys.*, **26**, 217 (1957).
(50) Lauterbur, P. C., private communication.
(51) Lide, D. R., and Mann, D. E., *J. Chem. Phys.*, **31**, 1129 (1959).
(52) Lipscomb, W. N., "Advances in Inorganic and Radiochemistry," Vol. I, Academic Press, Inc., New York, N. Y., 1959, p. 136.
(53) Lipscomb, W. N., *J. Chem. Phys.*, **22**, 985 (1954).
(54) Lipscomb, W. N., and Kaczmarczyk, A., *Proc. Natl. Acad. Sci.*, **47**, 1796 (1961).
(55) Lumley Jones, R., *J. Mol. Spectroscopy*, **2**, 581 (1958).
(56) Maher, J. P. and Evans, D. F., *Proc. Chem. Soc.*, 208 (1961).
(57) Manatt, S. L., and Elleman, D. D., *J. Am. Chem. Soc.*, **83**, 4095 (1961).
(58) Manatt, S. L., and Elleman, D. D., *J. Am. Chem. Soc.*, to be published.
(59) Manatt, S. L., and Elleman, D. D., *J. Am. Chem. Soc.*, **84**, 1579 (1962).
(60) Manatt, S. L., and Elleman, D. D., Research Summary No. 36-8, Jet Propulsion Laboratory, Pasadena, Calif., 1961, p. 74–77.
(61) Noggle, J. H., and Baldeschwieler, J. D., unpublished work.
(62) Ogg, R. A., *J. Chem. Phys.*, **22**, 1933 (1954).
(63) Ogg, R. A., and Ray, J. D., *Discussions Faraday Soc.*, **19**, 239 (1955).
(64) Overhauser, A. W., *Phys. Rev.*, **92**, 411 (1953).
(65) Piette, L. H., Ray, J. D., and Ogg, R. A., *J. Mol. Spectroscopy*, **2**, 66 (1958).
(66) Pople, J. A., and Shaefer, T., *Mol. Phys.*, **3**, 547 (1960).
(67) Pople, J. A., Schneider, W. G., and Bernstein, H. J., "High Resolution Nuclear Magnetic Resonance," McGraw-Hill Book Co., Inc., New York, N. Y., 1959, p. 31.
(68) Pople, J. A., Schneider, W. G., and Bernstein, H. J., Reference 67, p. 106.
(69) Pople, J. A., Schneider, W. G., and Bernstein, H. J., Reference 67, p. 116.
(70) Pople, S. A., Schneider, W. G., and Bernstein, H. J., Reference 67, Chap. 6.
(71) Pople, J. A., Schneider, W. G., and Bernstein, H. J., Reference 67, Chap. 10.
(72) Poss, H. L., *Phys. Rev.*, **75**, 600 (1949).
(73) Pound, R. V., *Rev. Sci. Instr.*, **28**, 966 (1957).
(74) Powles, J. G., *Reports Prog. Phys.*, **22**, 433 (1959).
(75) Price, W. C., *J. Chem. Phys.*, **16**, 894 (1948).
(76) Price, W. C., *J. Chem. Phys.*, **17**, 1044 (1949).
(77) Primas, H., Fifth European Congress on Molecular Spectroscopy, Amsterdam, 1961.
(78) Rabi, I. I., Ramsey, N. F., and Schwinger, J., *Rev. Mod. Phys.*, **26**, 167 (1954).
(79) Ramsey, N. F., *Phys. Rev.*, **100**, 1191 (1955).
(80) Randall, E. W., and Baldeschwieler, J. D., *J. Mol. Spectroscopy*, **8**, 365 (1962).
(81) Randall, E. W., and Baldeschwieler, J. D., *Proc. Chem. Soc.*, 303 (1961).
(82) Randall, E. W., and Baldeschwieler, J. D., unpublished work.
(83) Rigden, J. S., Hopkins, R. C., and Baldeschwieler, J. D., *J. Chem. Phys.*, **35**, 1532 (1961).
(84) Royden, V., *Phys. Rev.*, **96**, 543 (1954).
(85) Sanborn, R. H., *J. Chem. Phys.*, **33**, 1855 (1960).
(86) Schaeffer, R., Shoolery, J. N., and Jones, R., *J. Am. Chem. Soc.*, **79**, 4606 (1957).
(87) Schaeffer, R., Shoolery, J. N., and Jones, R., *J. Am. Chem. Soc.*, **80**, 2670 (1958).
(88) Schiff, L. I., "Quantum Mechanics," McGraw–Hill Book Co., Inc., New York, N. Y., 1955, p. 201.
(89) Schlesinger, H. I., Sanderson, R. T., and Burg, A. B., *J. Am. Chem. Soc.*, **62**, 3421 (1940).
(90) Schneider, W. G., Bernstein, H. J., and Pople, J. A., *Ann. N. Y. Acad. Sci.*, **70**, 806 (1958).
(91) Schneider, W. G., Bernstein, H. J., and Pople, J. A., *Can. J. Chem.*, **35**, 1487 (1957).
(92) Shimizu, H., and Fujiwara, S., *J. Chem. Phys.*, **34**, 1501 (1961).
(93) Shoolery, J. N., *Discussions Faraday Soc.*, **19**, 215 (1955).
(94) Shoolery, J. N., "This is N.M.R. at Work," No. 50, Varian Associates, Palo Alto, Calif.
(95) Shoolery, J. N., private communication.
(96) Smith, I. C., and Schneider, W. G., *Can. J. Chem.*, **39**, 1158 (1961).
(97) Solomon, I., *Phys. Rev.*, **99**, 559 (1955).

(98) Solomon, I., and Bloembergen, N., *J. Chem. Phys.*, **25**, 261 (1956).
(99) Sunners, B., Piette, L. H., and Schneider, W. G., *Can. J. Chem.*, **38**, 681 (1960).
(100) Snyder, E. I., and Roberts, J. D., *J. Am. Chem. Soc.*, **84**, 1582 (1962).
(101) Tomita, K., *Progress Theoretical Phys.* (Kyoto), **20**, 743 (1958).
(102) Turner, D. W., *J. Chem. Soc.*, 847 (1962).
(103) Vinogradov, S. N., and Linnell, R. H., *J. Chem. Phys.*, **23**, 93 (1955).
(104) Wangness, R. K., and Bloch, F., *Phys. Rev.*, **89**, 728 (1953).
(105) Waugh, J. S., and Dobbs, F. W., *J. Chem. Phys.*, **31**, 1235 (1959).
(106) Williams, R. E., Gibbins, S. G., and Shapiro, I., *J. Am. Chem. Soc.*, **81**, 6164 (1959).
(107) Williams, R. E., and Shapiro, I., *J. Chem. Phys.*, **29**, 677 (1958).